Tectonophysics 614 (2014) 146–169

Contents lists available at ScienceDirect

Tectonophysics

journal homepage: www.elsevier.com/locate/tecto

Crustal and lithospheric scale structures of the Precambrian Superior–Grenville margin

Ademola Q. Adetunji [a], Ian J. Ferguson [a,*], Alan G. Jones [b]

[a] Department of Geological Sciences, University of Manitoba, Winnipeg, Canada
[b] Dublin Institute for Advanced Studies, Dublin, Ireland

ARTICLE INFO

Article history:
Received 12 June 2013
Received in revised form 26 November 2013
Accepted 19 December 2013
Available online 29 December 2013

Keywords:
Grenville Province
Superior Province
Magnetotellurics
Geoelectric strike
Conductor
Lithosphere

ABSTRACT

The lithosphere beneath the margin of the Archean Superior and Proterozoic Grenville provinces was investigated with a northwest–southeast oriented, 650-km-long profile of 40 magnetotelluric stations. Dominant geoelectric strike azimuths of N45°E and N85°E were defined for the crust and the lithospheric mantle respectively. A 2-D isotropic resistivity model derived using the crustal strike images resistive Laurentian margin rocks dipping southeast to the base of the crust, bounded to the northwest by the Grenville Front, and to the southeast by the Central Metasedimentary Belt Boundary Zone. The observation is in contrast to conductive mid to lower crust elsewhere in the region. A 2-D isotropic resistivity model determined using the lithospheric mantle strike azimuth reveals an extremely resistive region in the upper 100 km of the mantle lithosphere of the northern Grenville Province. The geometry of this body, which includes a well-defined base and southeast dip, suggests that it is Superior lithosphere. A sub-vertical conductor, located approximately 50 km along strike from the Mesozoic Kirkland Lake and Cobalt kimberlite fields, is interpreted to be due to re-fertilization of an older mantle scar. The resistivity model includes a horizontal conductor at 160 km depth beneath the southern Superior Province that is possibly the resistivity signature of the lithospheric–asthenospheric boundary.

1. Introduction

POLARIS (Portable Observatories for Lithospheric Analysis and Research Investigating Seismicity) is a multi-institutional geophysical consortium focused on investigation of the structure and dynamics of the Earth's lithosphere, assessment of earthquake, and geomagnetic hazards across Canada, using the magnetotelluric (MT) method and earthquake seismology (Eaton et al., 2005). Between 2002 and 2005 seismic and MT data were collected in POLARIS study areas across Canada, including southern Ontario (Fig. 1). The focus of the Ontario MT study is to use deep electrical resistivity imaging to derive new geophysical and geological information on crustal and upper mantle structures and processes in the Grenville Province. MT results from the POLARIS projects in British Columbia, Manitoba, and southern Ontario have been presented by Soyer and Unsworth (2006), Gowan et al. (2009) and Frederiksen et al. (2006) respectively.

The MT method involves measuring the time-varying fluctuations of the natural electric and magnetic fields of the Earth and analyzing these data to map the spatial variation of the Earth's subsurface electrical properties. Signals with long periods (low frequencies) penetrate deeper into the Earth allowing the variation of resistivity with depth to be determined (Cagniard, 1953; Tikhonov, 1950). The subsurface resistivity structure can provide information on the processes that have formed and deformed a region (e.g., Evans et al., 2011; Ferguson et al., 2012; Jones, 1999; Jones and Craven, 1990; Miensopust et al., 2011; Nover et al., 1998; Spratt et al., 2009) and on the source of major conductivity anomalies (e.g., Ferguson et al., 2005; Jones and Savage, 1986). Enhanced electrical conductivity (reduced resistivity) in the crust is often linked to the presence and mobility of aqueous fluids (e.g., Glover and Vine, 1995; Hyndman et al., 1993). Graphite, interconnected grains of metallic oxides and sulfides are also important sources (e.g., Jones and Craven, 1990; Katsube and Mareschal, 1993; Li et al., 2003). There are several sources of enhanced electrical conductivity in the mantle, including graphite, hydrogen, partial melt, water and temperature variation (e.g., Constable, 2006; Ducea and Park, 2000; Hirth et al., 2000; Jones, 1999; Karato, 1990; Korja, 2007; Mibe et al., 1998; Muller et al., 2009; Selway, 2013; Yoshino et al., 2008).

The electrical resistivity structure of the Grenville Front (GF) region and the southern subprovinces of the Superior craton has been examined in earlier MT studies (Boerner et al., 2000) but there have been very few MT studies in areas south of the GF (e.g., Kurtz, 1982). Previous results for the GF area were derived mainly from 1-D inversion and 2-D forward modeling. They showed that the upper crust is generally resistive, the middle to lower crust is relatively conductive, and the uppermost mantle is resistive (Kellett et al., 1992; Kurtz, 1982; Zhang et al., 1995).

Results from the previous MT studies have been interpreted as indicating anisotropic electrical resistivity within the mantle in the GF area

* Corresponding author at: Department of Geological Sciences, University of Manitoba, Winnipeg, MB R3T 2N2, Canada. Tel.: +1 204 474 9154; fax: +1 204 474 7632.
E-mail address: IJ_Ferguson@umanitoba.ca (I.J. Ferguson).

0040-1951/$ – see front matter © 2014 Elsevier B.V. All rights reserved.
http://dx.doi.org/10.1016/j.tecto.2013.12.008

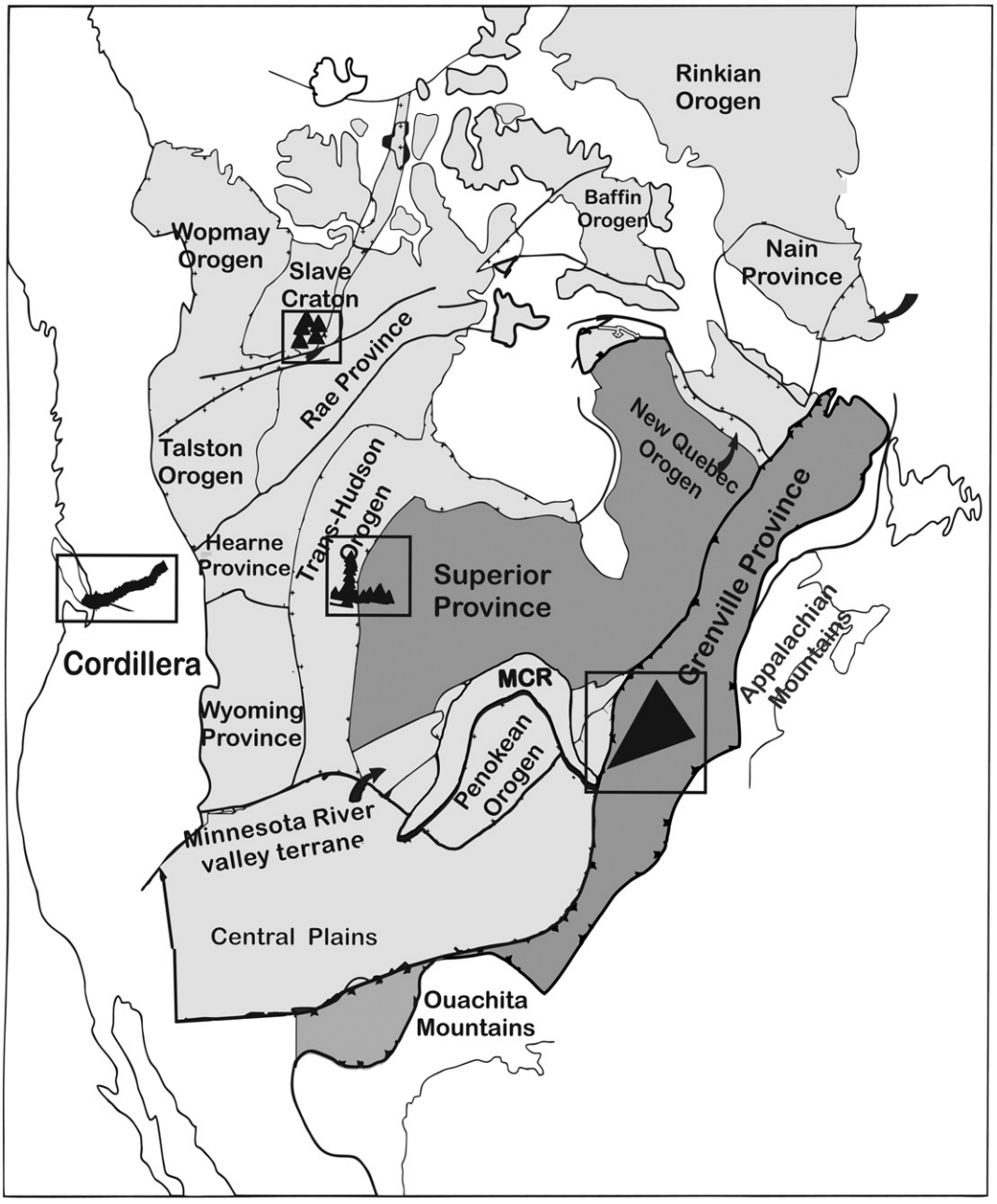

Fig. 1. Initial deployments of POLARIS MT sites in Canada. The first four POLARIS deployments were in the Cordillera, Slave craton, Superior craton–Trans Hudson Orogen margin, and the Grenville Province. Tectonic background modified from Hoffman (1989). MCR = mid-continent rift.

(e.g., Frederiksen et al., 2006; Ji et al., 1996; Kellett et al., 1992; Mareschal et al., 1995). The interpretation of the observed azimuthally-dependent MT responses in terms of anisotropy was based on the absence of induction arrow responses that would be indicative of 2-D or 3-D structures. The anisotropy was constrained to lie between 45 and 150 km depth (Mareschal et al., 1995) and interpreted to be associated with southward extension of Archean Superior rocks beneath the Grenville Province (Boerner et al., 2000; Kellett et al., 1992). Ji et al. (1996) suggested that the anisotropy is caused by shape-preferred orientation of mantle minerals.

The present study area includes the Abitibi and Pontiac Subprovinces of the Archean Superior Province and the Central Gneiss Belt (CGB) as well as the Central Metasedimentary Belt (CMB) of the Proterozoic Grenville Province (Fig. 2). It describes the processing and interpretation of MT data along a profile oriented in a northwest–southeast direction that extends the earlier Lithoprobe Abitibi–Grenville Transect MT acquisition (Boerner et al., 2000) with POLARIS MT (Eaton et al., 2005) stations. It contrasts with the prior MT studies of the Superior–Grenville margin (e.g., Ji et al., 1996; Kellett et al., 1992; Mareschal et al., 1995) by using full 2-D inversion methods to model the MT data. The profile of MT stations examined in this study provides the highest available density of MT sites crossing the Superior–Grenville boundary. However, additional MT data have been collected in the Superior–Grenville area in the Lithoprobe and POLARIS projects. Results from a larger-scale study area are examined in Adetunji et al. (in preparation) which also include a more detailed examination of local and regional geoelectric strike variation, tipper responses, and MT tensor distortion in the Superior–Grenville area.

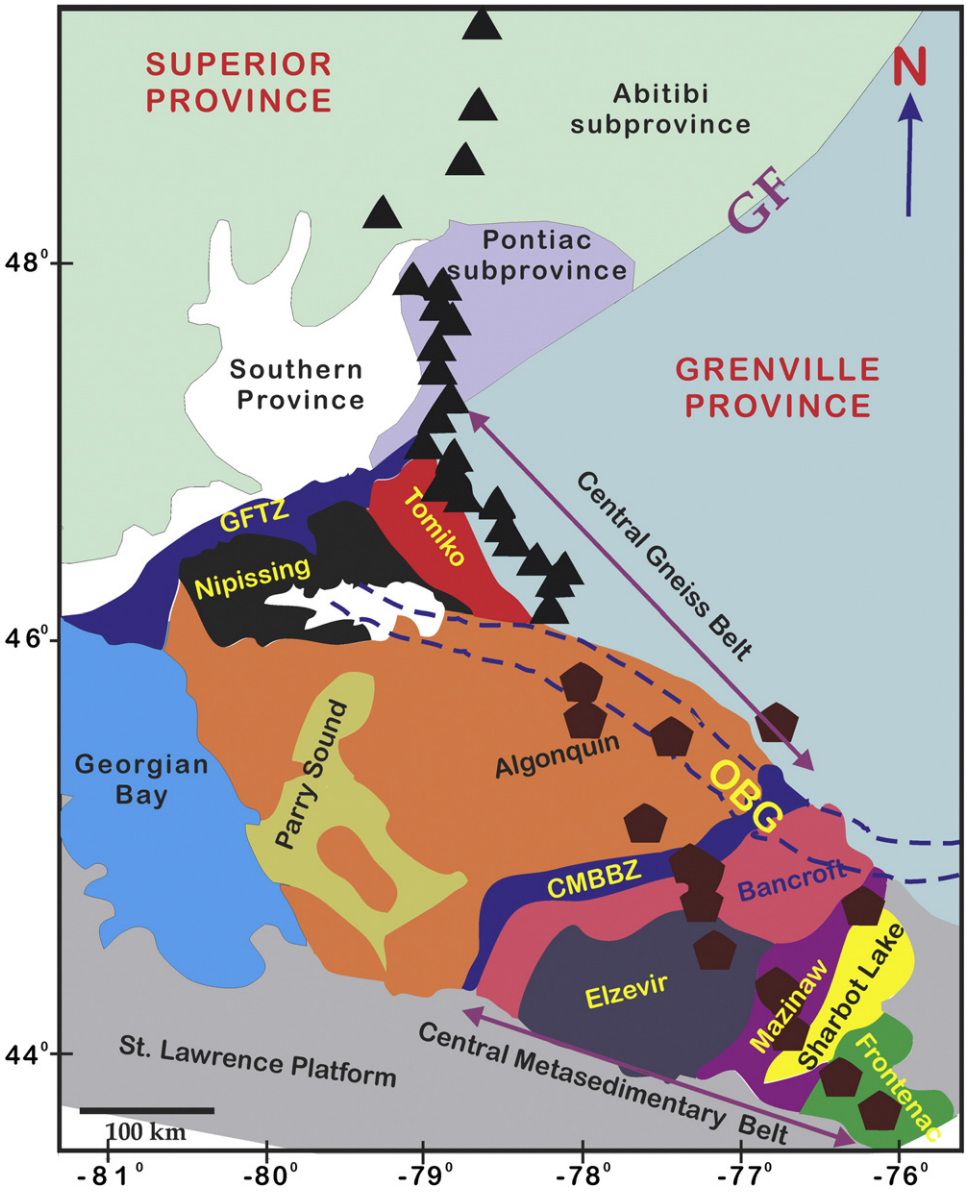

Fig. 2. A simplified geotectonic map of the study area showing the location of the MT sites. Triangles represent the LITHOPROBE Abitibi–Grenville transect MT sites and polygons represent the POLARIS MT sites. Sub-units of the Superior and Grenville Provinces are labeled. GF = Grenville Front, GFTZ = Grenville Front Tectonic Zone, OBG = Ottawa Bonnechere Graben; CMBBZ = Central Metasedimentary Belt Boundary Zone.

2. Geological and tectonic setting

The Archean Superior Province mostly comprises rocks formed between 2.8 and 2.7 Ga (Hoffman, 1989). The Abitibi Subprovince represents a remnant from a larger Neoarchean granite–greenstone terrain that has a record of rapid crustal growth during the Neoarchean (Card, 1990; Percival et al., 2004). It is characterized by polycyclic volcanic stratigraphy overlain by a late-stage sequence of turbiditic sedimentary rocks and synorogenic clastic rocks. Numerous granitoid plutons intruded and deformed these rocks in several phases of folding and faulting (Card and Poulsen, 1998).

The Pontiac Subprovince is an Archean metasedimentary and plutonic terrane separated from the Abitibi Greenstone Belt to the north by the Cadillac Larder–Lake Fault Zone (CLLFZ); while to the south its boundary with the Grenville Province is marked by the southeast-dipping Grenville Front Tectonic Zone (GFTZ) (Card and Ciesielski, 1986). It is characterized by supracrustal, metagraywacke and metasedimentary rocks together with a small metavolcanic belt (Card, 1990; Card and Poulsen, 1998; Dimroth et al., 1982).

The Grenville Province was formed during middle to Late Mesoproterozoic orogenic activity (Easton, 1992; Hanmer, 1988; Hoffman, 1989). The orogen followed a period of pre-Grenvillian continental-margin arc magmatism, accretionary, and collisional tectonic events (Carr et al., 2000). This collision and thrusting resulted in a first phase of high grade metamorphism and convergent deformation, which occurred between 1190 and 1140 Ma (Corrigan and van Breemen, 1997; Rivers et al., 1989). In southwestern Ontario, the Grenville orogen produced northwest-trending thrusting of a composite belt of continental crustal and magmatic rocks onto the margin of the Laurentian craton (Carr et al., 2000; Rivers, 1997). The collisional tectonics resulted in crustal thickening, and local over-thickening due to the ductile nature of the crust (Ludden and Hynes, 2000). This was followed by orogenic collapse and emplacement of mantle- and lower-crustal-derived magmas.

The GFTZ marks the northwestern boundary of the Grenville orogen and thrusting along this shear zone occurred late in the Grenvillian orogeny, at ca. 990 Ma (Haggart et al., 1993; Krogh, 1994). The GFTZ is a prominent southeast-dipping crustal-scale shear zone of amphibolite-

facies rocks. Its boundaries are gradational and are deformed by cataclastic zones that extend into the adjacent Superior Province (Easton, 1992).

Division of the Grenville Province into the CGB in the north and the CMB to the south is based on the contrasting lithologies of these terranes (Easton, 1992) and we use these terminologies herein. More recently, the CGB has been referred to as part of pre-Grenvillian Laurentia and its margin, and the constituent units of the CMB, with the exception of the Frontenac terrane, have been collectively termed the Composite Arc belt (e.g., Carr et al., 2000).

The CGB represents the reworked margin of the pre-Grenvillian Laurentian craton (Carr et al., 2000). It is characterized by layered felsic gneiss and amphibolites, and upper amphibolite to granulite facies plutonic and supracrustal rocks (Easton, 1992). Several ductile shear zones that separate distinctive lithotectonic domains and sub-domains in the CGB show an indication of a northwest-directed low angle ductile thrusting (Davidson, 1986). This belt is subdivided into four (Nipissing, Algonquin, Tomiko and Parry Sound) domains (Fig. 2) based on contrasting lithologies, metamorphic grade and deformation histories. These domains represent imbricated panels of relatively low strain rocks bounded by anastomosing ductile shear zones (e.g., Culshaw et al., 1983; Davidson and Morgan, 1981; Davidson et al., 1982; Hanmer and Ciesielski, 1984).

The CMB lies to the southeast of the CGB from which it is separated by the Central Metasedimentary Boundary Belt Zone (CMBBZ). Shear indicators in this zone indicate thrusting of the CMB northwestwardly against the CGB (Davidson, 1998; Easton, 1992). The CMBBZ is characterized by alternating crystalline thrust sheets enveloped by anastomosing higher strain zones of porphyroclastic to migmatitic tectonites and marble tectonic melange (Hanmer and McEachern, 1992; Hanmer et al., 1985).

The CMB contains a major accumulation of carbonate, siliciclastic, plutonic, and volcanic rocks metamorphosed into greenschist to granulite facies during the Grenvillian orogeny (Easton, 1992; White et al., 2000). The rocks of the CMB are dominated by structural polyfolded domains with complex geometry (White et al., 2000). Based on different lithologies, metamorphic grade, deformation and geochronological histories, the CMB is subdivided into five domains (Fig. 2): the Bancroft, Elzevir, Mazinaw, Sharbot Lake and Frontenac terranes.

The Ottawa Bonnechere Graben is a 60 km wide graben (Mereu et al., 1986) that lies along the border between Ontario and Quebec (Fig. 2). This graben has been interpreted as a failed arm of a triple junction formed during a late Precambrian to early Paleozoic event during which the Iapetus ocean opened (Kamo et al., 1995; Kumarapeli, 1985). It consists of deformed metasedimentary and metavolcanic rocks intruded by felsic to mafic plutons (Easton, 1992).

The youngest tectonic event associated with the study area is the interpreted Great Meteor hotspot (Crough, 1981; Sleep, 1990). The track of this hotspot was interpreted to be responsible for the emplacement of the Cretaceous Monteregian–White Mountain–New England Seamounts Igneous Province (Crough, 1981; Sleep, 1990). It is also interpreted to be associated with the Mesozoic lamprophyric dykes and kimberlite magmatism at Rapide des Quinze (Ji et al., 1996) and Kirkland Lake (Ji et al., 1996; Meyer et al., 1994) areas of Pontiac Subprovince (Faure et al., 2011; Griffin et al., 2004).

3. MT data

In the POLARIS project, MT data were collected at a total of 41 sites within the southern Ontario POLARIS array between 2002 and 2005 (Eaton et al., 2005). These sites include 20 broadband MT (BBMT), 7 long period MT (LMT) and 14 LMT + BBMT sites distributed across the Grenville Province in southern Ontario. The MT data examined in this study are from 40 Lithoprobe and POLARIS broadband MT sites on a northwest–southeast, 650-km-long profile (Fig. 2). Twenty-five Lithoprobe stations (triangles in Fig. 2) extend from the Abitibi Subprovince to the CGB while 15 POLARIS stations (pentagons in Fig. 2) cross part of the CGB and the entire CMB. The POLARIS sites also cross the Ottawa Bonnechere Graben. The data from the Lithoprobe Abitibi–Grenville Transect studies have been described in Boerner et al. (2000), Ji et al. (1996), Kellett et al. (1992), Mareschal et al. (1995), Sénéchal et al. (1996), and Zhang et al. (1995). The POLARIS data are described in Adetunji (2013) and Frederiksen et al. (2006).

A resistivity structure may be 1-D or horizontally-layered, 2-D with a geoelectric strike in which the resistivity is invariant, or it may have a more complex 3-D form. The primary responses derived from the MT data are the apparent resistivity and impedance phase; both responses provide information on the underlying resistivity structure (Chave and Jones, 2012; Vozoff, 1991). The MT responses measured over a 2-D structure are the transverse electric (TE) mode in which the electric field is parallel to the geoelectric strike, and the transverse magnetic (TM) modes in which the electric field is perpendicular to the strike. The depth of penetration of MT signals depends on both the period of the signal and the local resistivity. The maximum depth of penetration of the responses in the present study was estimated for each site with the Niblett–Bostick depth transform (Jones, 1983; Niblett and Sayn-Wittgenstein, 1960) of the TE and TM modes of best-fitting regional 2-D responses. Although the estimated depths might be affected to some degree by 3-D effects, the Niblett–Bostick approximation provides a superior method for comparing related responses than a period-based data analyses (Jones, 2006). At all of the MT sites considered in the present study, the maximum period of responses is 1820 s and depending on the local resistivity, this period corresponds to a depth of between 100 km and 400 km (Fig. 3). The penetration depth differs at the same site for different modes, an effect discussed in Jones (2006).

4. Geoelectric dimensionality and strike analysis

Galvanic distortion of the electric field by near-surface inhomogeneities can mask the true dimensionality of the regional resistivity structure unless tensor decomposition methods are applied to remove its effects (e.g., Bahr, 1988; Caldwell et al., 2004; Groom and Bailey, 1989; Jones, 2012; McNeice and Jones, 2001). In this study the galvanic distortion and geoelectric strike were determined using the single-site STRIKE algorithm of McNeice and Jones (2001) that is based on the Groom and Bailey (GB) tensor decomposition (Groom and Bailey, 1989, 1991). The GB method fits a regional 2-D MT response in the presence of in-phase frequency-independent electric field distortion. McNeice and Jones (2001) extended the GB method to multi-site and multi-frequency fitting which allows for the determination of the optimal strike for a group of sites and/or a selected range of frequencies. A more recent modification involves the determination of strike azimuth for a specified depth range using Niblett–Bostick depth approximation (e.g.; Hamilton et al., 2006; Miensopust et al., 2011; Muller et al., 2009). This approach greatly reduces the mixing of strikes from different depths, which, because of the resistivity dependent depth of MT signal penetration, can occur in frequency-based studies (Jones, 2006). As indicated in Fig. 3, there is a strong variation in the penetration depth of the MT responses along the profile, and this supports the use of depth-bands in the geoelectric strike analyses.

In the present study, depth is divided into nominal crustal (1–40 km), lithospheric mantle (40–200 km) and asthenospheric mantle (200–400 km) ranges. These depth bands are based on a priori information rather than on MT results. The crustal depth range was defined so as to exclude near-surface structures, and the crust–mantle depth was based on seismic estimates of the depth to the Moho (Eaton et al., 2006; White et al., 2000). The lithospheric mantle depth range is based on typical lithospheric thickness defined by Artemieva (2009), while the asthenospheric depth range includes all deeper-penetrating periods. The results of the geoelectric strike estimation, presented in this paper, were based on an impedance error floor of 3.5%,

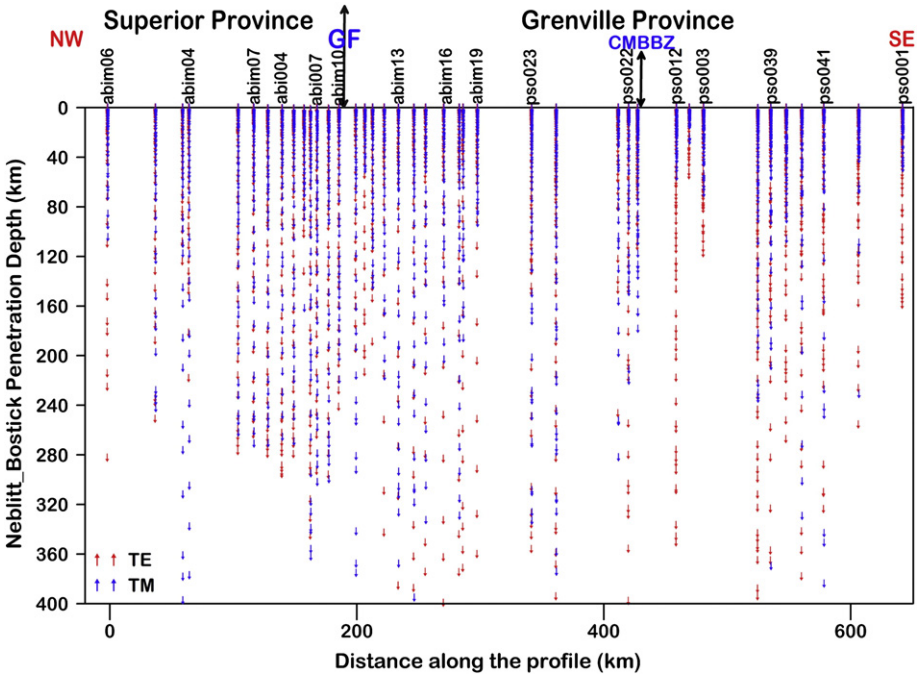

Fig. 3. The Niblett–Bostick penetration depth for the 40 sites on the profile. Each of the symbols represents the response at a particular period. Red color represents penetration depth for TE mode and blue color represents penetration depth for TM mode. GF = Grenville Front; CMBBZ = Central Metasedimentary Belt Boundary Zone.

which corresponds to a 7% error for the apparent resistivity and 2° for phase.

In GB tensor decomposition, galvanic distortion is parameterized in terms of shear that defines the polarization of the electric field and twist that defines its rotation (Groom and Bailey, 1989, 1991). The root mean square (RMS) misfit of the GB model provides a measure of the fit to the observed response of the GB model. The shear and twist angles, as well as the RMS misfits, for each site are shown in Fig. 4. The results indicate that there is a moderate level of distortion in the study area. For the crustal depth range, the mean of the absolute value of the shear angle is 19° and the mean of the absolute value of the twist is 12° (with a standard deviation of 12° in both cases). The absolute values of the shear and twist angles are predominantly <25° and <15° respectively. For the lithospheric mantle depth range (Fig. 4b and d), the mean of the corresponding absolute values of shear and twist values is 24° and 18° (with standard deviation of 14° in both cases). Variogram analysis of the results indicates that the shear and twist responses are dominated by local rather than regional effects (Frederiksen et al., 2006).

The distribution of the RMS misfits for the crustal (Fig. 4e) and the lithospheric mantle (Fig. 4f) depths shows that most of the sites have an average RMS misfit of less than 2.0, which is considered to be an acceptable value (Jones, 2012), with a peak mode of ~0.75 for both the crust and the mantle lithosphere. The sites with high RMS misfit are mainly located near major shear zones (the GF and CMBBZ).

Fig. 5 shows Rose diagrams of geoelectric strike azimuths for crustal, lithospheric mantle and asthenospheric mantle depths. The 90° ambiguity that normally affects geoelectric strike determination (e.g., Hamilton et al., 2006) was addressed by plotting results in a single quadrant (azimuth of 10°–100°) that includes the surface geological strike. The dominant geoelectric strikes are N45°E for the crust (Fig. 5a), N85°E for the lithospheric mantle (Fig. 5b) and N68°E for the asthenospheric mantle (Fig. 5c).

At lithospheric mantle depths, most of the strike azimuths lie between N75°E and N90°E with some local deviations within the Pontiac Subprovince and near the CMB. The regional lithospheric mantle strike determined in this study generally agrees with the N80°E ± 6° obtained by Ji et al. (1996) and the results of Frederiksen et al. (2006). The differences are due to variation in the number of data used and the method of computation; this study is based on depth-transformed data whereas previous studies were based on periods. Data from only seventeen sites within the study area provide penetration to mantle depths exceeding 200 km. They show geoelectric strike direction that ranges from N60°E to N75°E (Fig. 5c).

Fig. 6 shows the individual single-site GB strike azimuths for the crust (Fig. 6a) and the lithospheric mantle (Fig. 6b). At crustal depths, the majority of the sites have strike azimuths that are parallel to, or sub-parallel to, regional geological strike, e.g., as defined by the GF and CMBBZ. As noted in Frederiksen et al. (2006), strike azimuth at some sites is parallel to the local total magnetic field anomalies. However, at other sites, particularly within the CMB, the azimuth is not parallel to either the regional geological strike or local magnetic field anomalies.

At lithospheric mantle depths, except for a couple of local exceptions, the sites show a very consistent east–west strike direction. Over the whole length of the profile this azimuth is consistently 30° to 40° clockwise from the crustal azimuth. As previously observed by Mareschal et al. (1995) and Ji et al. (1996), the lithospheric mantle strike azimuth is very uniform in a region crossing the GF and extending in the CGB.

Fig. 6c shows the relationship between the individual single-site GB strike azimuths for the asthenospheric mantle depth. There is excellent agreement between the strike azimuths at most sites. The discrepancy at the remaining two sites may be due to the effects of noise or residual distortion in the MT data at these sites.

The consistency of geoelectric strike in the crust and the lithospheric mantle, along with the relatively low RMS misfit values, suggests that 2-D modeling is a reasonable approach for the determination of crustal and lithospheric mantle resistivity structures. However, the different average strike azimuths of N45°E (crust) and N85°E (lithospheric mantle) indicate the need for separate modeling at the two depths. Data sets were prepared for 2-D inversion using the regional responses from the GB decompositions with the regional geoelectric strike azimuth constrained to either the crust or lithospheric mantle value. The data set included the tipper response (T_z) which defines the relationship between the vertical and horizontal magnetic field components

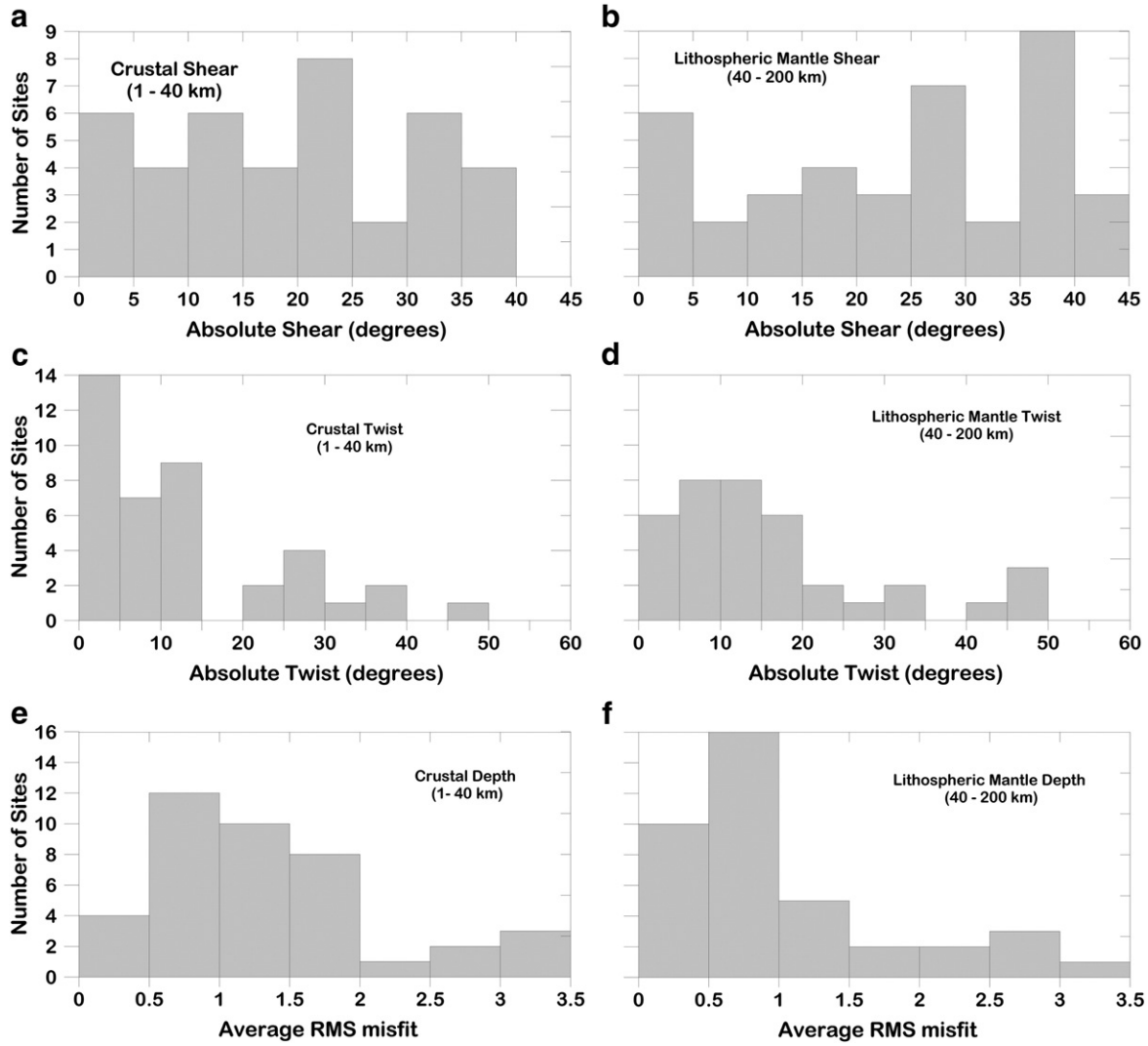

Fig. 4. Distribution of the absolute value of the shear and twist angles for the crustal (a and c) and the lithospheric mantle (b and d) depths. The distribution of the average RMS misfits for the crustal (e) and lithospheric mantle (f) depths are also shown.

and forms part of the TE mode response (Vozoff, 1991). Prior to 2-D inversion, the data sets were re-edited and examined using TE and TM pseudosections and tipper pseudosections. The D+ approach (Parker, 1980), which performs 1-D modeling of the admittance, was used to check for consistency between phase and apparent resistivity responses and to aid in identifying unreliable data points that were subsequently removed prior to modeling/inversion.

For 1-D and 2-D structures the impedance phase responses are related to the gradient of apparent resistivity with log period (e.g., Parker and Booker, 1996; Weidelt and Chave, 2012). Increasing phase values greater than 45° indicate increase in conductivity with depth, values close to 45° indicate relatively uniform conductivity with depth while decreasing values less than 45° indicate decrease in conductivity with depth. The phase response is a more robust response than the apparent resistivity and for 1-D and 2-D structures it can be recovered exactly from distorted responses using tensor decomposition methods. In contrast, after tensor decomposition the apparent resistivity may still be affected by static shift, a frequency-independent multiplicative factor (Jones, 1988).

The MT apparent resistivity and phase pseudosections for both the crustal and lithospheric mantle data sets are presented in Figs. 7 and 8 respectively. Apparent resistivity and phase responses for both TE and TM modes are examined in both cases and the results indicate that significant differences exist between the TE and TM responses, which indicate the presence of 2-D structures. The TE mode is sensitive to current flow, which is dictated by the conductance of conductive regions of the sub-surface, but has lower sensitivity to the lateral position of structures than TM mode. The TM response is sensitive to charges on conductivity contrasts or gradients of lateral boundaries. The pseudosections for the crustal and lithospheric mantle strike directions are generally very similar but there are some differences evident for the responses in the different strike directions.

The apparent resistivity response for both pseudosections is dominated along most of the profile by high values (>2000 Ω·m) over an intermediate period band between 10^{-3} and 1 s. This response extends from the northwestern end of the profile southeast to the middle of CMB where the resistivity in the band decreases to values of <20 Ω·m. At shorter periods the response is generally more conductive (<1000 Ω·m), although in the CGB, resistive responses are observed to extend to the shortest periods. The transition from the conductive to the resistive response, at the shortest to the intermediate periods (10^{-4} to 10^{-2} s), is reflected in the phase response by a region of low impedance phase (<30°). The apparent resistivity at longer periods (>1 s) is typically <500 Ω·m. The transition from high apparent resistivity at intermediate periods to lower apparent resistivity at long periods is reflected in a period band of high phase responses (>60°) centered on 1 s extending along most of the profile. These observations provide evidence for a structure extending over the profile that is

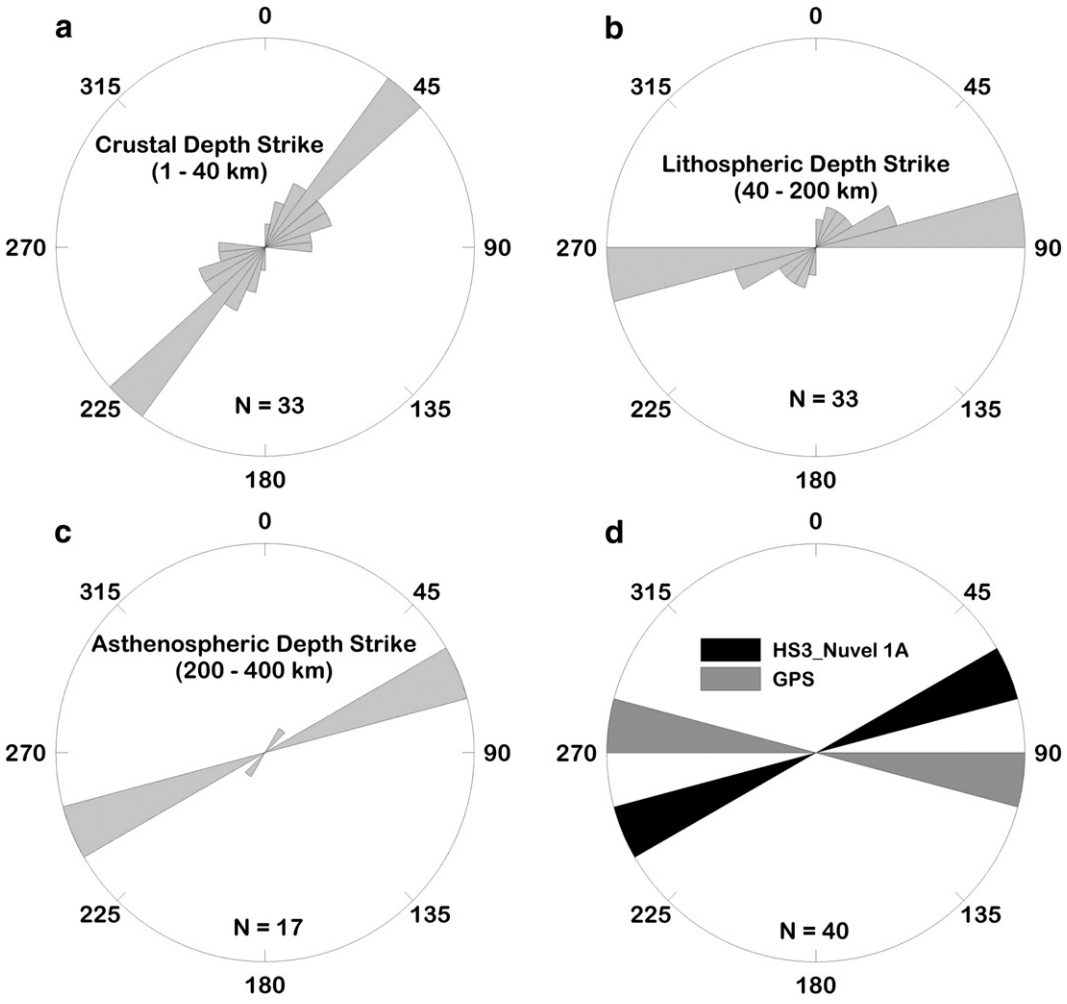

Fig. 5. Rose diagrams of the regional geoelectric strike for (a) crustal depth, (b) lithospheric depth, (c) asthenospheric depth and (d) the absolute plate motion for the HS3_Nuvel 1A hotspot model defined by Gripp and Gordon (2002) and for the GPS based model defined by Larson et al. (1997). The bin size in all cases is 15° and N denotes number of data points (sites) used for each plot.

relatively conductive near the surface, resistive at intermediate depths, and conductive at depth. Lateral variations in these responses, for example, increased TE mode apparent resistivity at intermediate periods in the CGB, indicate the presence of 2-D structures. In the CMB there are some differences in the form of the responses between the crust and lithospheric mantle pseudosections indicating the presence of strong 2-D structures.

The pseudosections provide evidence for several more conductive areas. In the northwestern part of the profile, there is a relatively conductive zone observed at short periods (~10^{-4} to 10^{-2} s). This zone extends from the Abitibi Subprovince into the middle of the CGB (Figs. 7 and 8). At the southeastern end of the profile, beneath the first site (PSO001), both pseudosections include a conductive zone defined by low apparent resistivity values in the TE and TM apparent resistivity responses at short periods. The lithospheric mantle apparent resistivity pseudosection (Fig. 8) includes a second conductive feature at longer periods at this location. Finally, there is a conductive response observed at long periods in the northwest of the profile in the lithospheric mantle strike pseudosection (Fig. 8). The response includes increased TM mode phase values at ~1000 s over the northwestern half of the profile. The phase values are locally higher in the part of the profile beneath the Pontiac Subprovince and at this location; there is an additional high-phase response in the TE component and a zone of decreased TM mode apparent resistivity.

The tipper data (not shown) were rotated to the 2-D modeling coordinate system, and the component parallel to the profile was edited carefully prior to inclusion in 2-D inversions. The tipper is usually sensitive to the local structures but can also be strongly affected by conductivity boundaries at the edges or outside of the region modeled. Based on visual inspection, the tipper data were heavily edited to exclude power-line effects and erratic points characterized by jumps in tipper magnitudes, tipper magnitudes exceeding 1, and/or large error estimates. In addition, based on the study of Zhang et al. (1993), short period (<0.1 s) tipper data were excluded because of the possible contamination by magnetic effects of galvanic distortion. Following the editing, the tipper responses include several large-scale spatial variations.

5. Two-dimensional modeling and inversion

The crust and lithospheric mantle in the study area were separately modeled using 2-D isotropic inversion of MT data decomposed to the appropriate strike directions for the two depth ranges. We used the 2-D isotropic modeling and inversion algorithm of Rodi and Mackie (2001), as implemented in Geosystem's (now Western Geco/Schlumberger) WinGLinK software. The 2-D forward modeling uses a finite difference numerical method for calculation. The inversion code applies the non-linear conjugate gradient (NLCG) method for direct iterative minimization of an objective function that penalizes data residuals and second spatial derivatives with respect to resistivity structures (Rodi and Mackie, 2001, 2012).

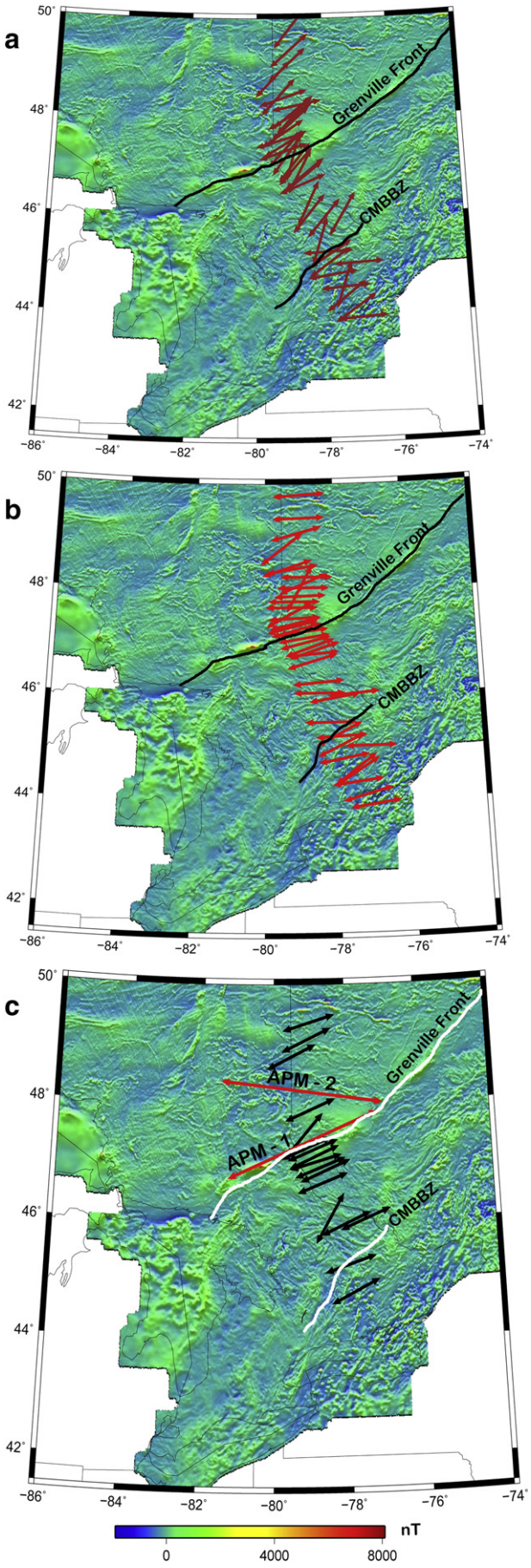

The inversion models were obtained by solving for the smoothest model using uniform-grid Laplacian regularization and minimizing the integral of the Laplacian (Rodi and Mackie, 2012). Many 2-D inversions, using different combinations of inversion parameters and data, were run to explore the range of possible models that could fit the data. Inversion of TE data alone resolves mainly the depth and the conductivity-thickness product of the conducting regions, whereas inversion of the TM data alone resolves their horizontal extent and the presence of resistive layers (Agarwal et al., 1993; Simpson and Bahr, 2005; Vozoff, 1991). Inclusion of both modes in the inversion allows for superior determination of the subsurface resistivity structure. All the 2-D models were derived using a 100 Ω·m half space as the starting model. Initial models were obtained by fitting the TE, TM and vertical magnetic transfer function for all 40 BBMT sites. Some highly distorted sites, with extreme RMS-misfits (>4.0), were later excluded from the final set of inversions.

The uncertainty estimate on each data point was set to either the calculated error value or to an error floor if the calculated error was smaller than the value of the error floor. When 2-D inversion methods are applied to data containing weak 3-D effects, error floors must be set appropriately. For example, when the conductive features in a model have a finite strike length, the TE response is generally more distorted than the TM response (Ledo et al., 2002). However, there are some geometries for which the TM mode is more affected by 3-D effects than the TE mode (e.g., Park and Mackie, 1997). In this study, for the initial set of inversions, error floors of 50% were set for the apparent resistivity of both modes, the error floor for TE phase was set at 25% and the error floor for TM phase at 5%. The apparent resistivity was down weighted in order to reduce the effect of static shift. All of the error floors were subsequently reduced to 16% and 12% for TE and TM apparent resistivity and 4% (~1.2°) and 3% (~1°) for TE and TM phases, respectively. The vertical magnetic transfer function (tipper) error was set at 0.02. The apparent resistivity data for the final set of models were corrected for static shift effects. Every new inversion was restarted at least once after its initial termination so that the final model would represent a deeper minimum of the objective function. The typical number of iterations per sequence was 400.

A range of weighting functions and regularization parameters were examined to explore for the optimal model (e.g., Mackie et al., 1997; Schäfer et al., 2011; Spratt et al., 2009). The model term in the objective function includes a multiplication factor α that is applied to the horizontal derivative and controls the relative horizontal smoothness of the inversion model. Another parameter, β, is an exponential factor that increases the weighting function with depth. Additional parameters that regulate the spatial smoothing are the minimum block dimension in the horizontal and vertical directions, H and V respectively. The Tikhonov regularization parameter (τ) controls the trade-off between RMS-misfit and model-roughness. Large τ results in smooth models with high RMS-misfit whereas small τ produces a good fit to the data but rough structures are required. The optimal value of τ was determined by plotting a trade-off (L) curve between the regularization parameter and the RMS-misfit. The inversions used for this purpose were mainly based on the phase responses. For both the crustal and lithospheric mantle data sets, $\tau = 6$ gave results in the elbow of the trade-off curve providing a relatively good data fit and a relatively smooth model. Other weighting function parameters were set at $\alpha = 1$, $\beta = 0.3$, $H = 500$ and $V = 500$ for the inversions. These values were chosen after a series of initial inversions that were performed to determine the best smoothing and regularization parameters.

Fig. 6. The crustal (a), lithospheric mantle (b) and the asthenospheric mantle (c) strike azimuths obtained from the STRIKE program with 90° ambiguity correction are plotted on the regional magnetic map (data obtained from Geological Survey of Canada). The longer arrow, APM-1, shows the HS3-Nuvel-1A absolute plate motion direction defined by the hotspot based model of Gripp and Gordon (2002) and the arrow APM-2 shows the absolute plate motion of the GPS based model of Larson et al. (1997).

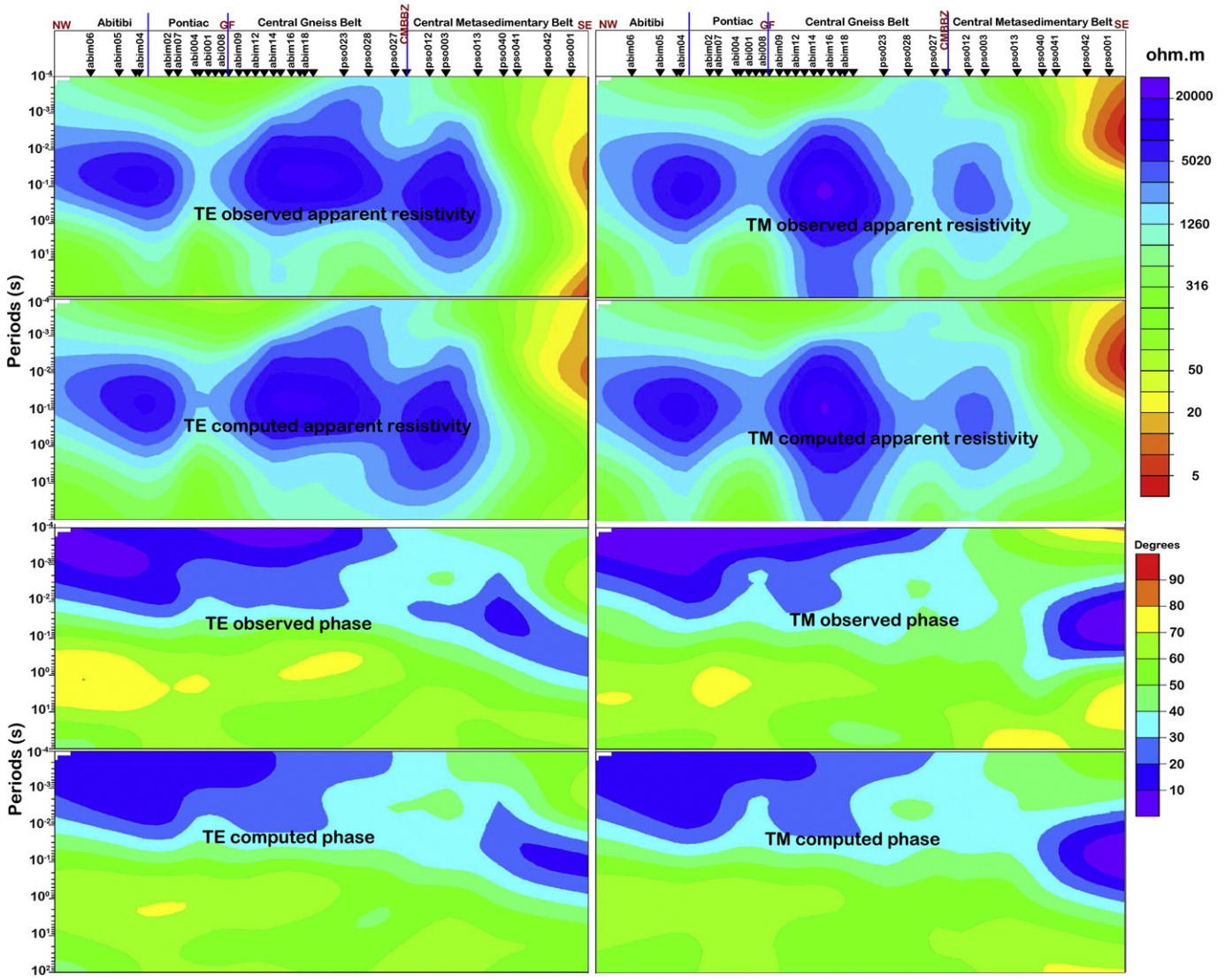

Fig. 7. The apparent resistivity and phase pseudosections of TE and TM responses for the study area. The data are the regional impedances derived from the GB decomposition for the crustal strike azimuth of 45°. Each panel shows the observed responses and the responses of the 2-D resistivity model fitted to the observed data. Static shift correction has been applied to the apparent resistivity responses.

Fig. 8 compares the model response pseudosections with the data pseudosections for the best-fitting model of lithospheric mantle data set, and Fig. 9 compares the observed TE, TM and tipper responses with the modeled ones at representative sites in the study area. The data fit is considered acceptable for all the sites shown, with individual RMS values of <2. The misfit at other sites is shown in Figs. 10 and 11 for the crustal and lithospheric models respectively. The overall fit to the tipper response is poorer than the fit to the MT apparent resistivity and phase responses, but examination of the real and imaginary pseudosections of the tipper (not shown) shows that the model reproduces the large-scale features of the observed data.

5.1. Crustal resistivity model

Fig. 10 shows the final crustal 2-D resistivity model from simultaneously inverting the TE + TM + Tz data. The RMS-misfits of the separate TE (red), TM (blue) and joint TE + TM + Tz (purple) inversions, for each of the sites, are shown at the top of the model. The data fit is relatively good to the northwest of the CMBBZ, where the average misfit for the joint inversion is around 2. The misfit is particularly poor at some sites within the CMB, which is attributed in part to the structurally complex metasedimentary rocks that occur in this region. However, the global RMS misfit value of 2.4 is considered acceptable in light of the distribution of the misfit, and inspection of the data versus model pseudosections indicates that no major data feature is being misfit.

The resistivity structures defined by the joint and individual inversions reveal some differences caused by the different sensitivities of the different modes. Generally, the crustal model shows that there is a resistive upper crust below a relatively thin conductive layer near the surface. The resistive crust extends to 8–10 km depth beneath the Abitibi and Pontiac subprovinces (Feature A in Fig. 10). The Superior Province is characterized by very resistive upper crust (>10,000 Ω·m), with resistivity decreasing with increasing depth. The resistive zone extends to 16–20 km depth beneath the CGB and northwestern part of the CMB (Feature D). A well-resolved resistive zone (Feature B), including resistivity exceeding 10,000 Ω·m, dips southeast to the base of crust beneath the CMBBZ. The resistive zone is <5 km thick in the southeastern part of the CMB and is less resistive than further to the northwest.

Except for the resistor beneath the CMBBZ, the middle to lower crust is relatively conductive, <500 Ω·m, along the whole profile. A poorly-resolved localized conductive zone (Feature C) (~30 Ω·m) is imaged in the upper crust beneath the CMBBZ. The southern end of the profile is characterized by a fairly well resolved conductive zone in the lower crust (Feature E) (<10 Ω·m) that is defined by the data at the two

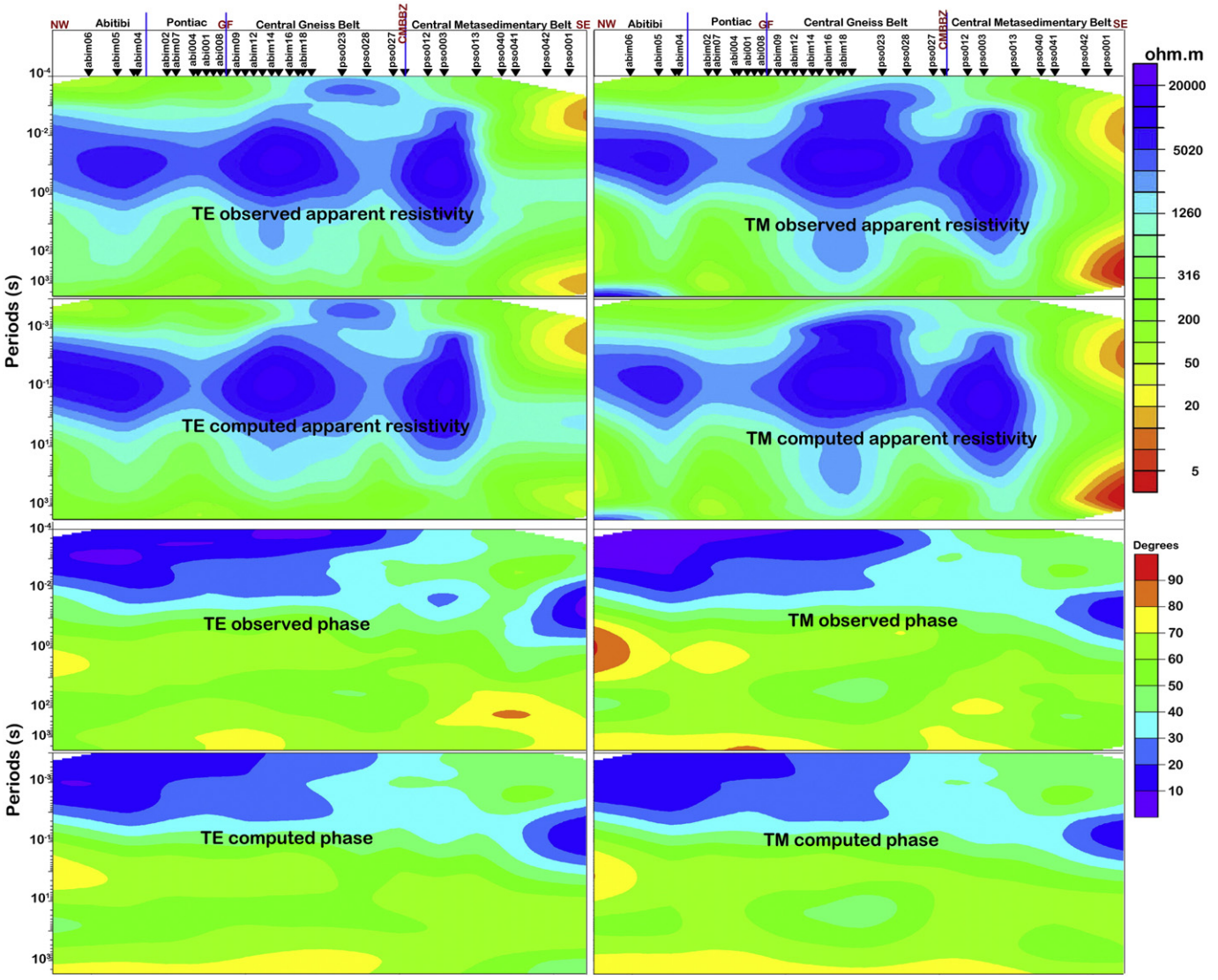

Fig. 8. The apparent resistivity and phase pseudosections of TE and TM responses for the study area. The data are the regional impedances derived from the GB decomposition for the lithospheric mantle strike azimuth of 85°. Each panel shows the observed responses and the responses of the 2-D resistivity model fitted to the observed data. Static shift correction has been applied to the apparent resistivity responses.

southeasternmost sites (PSO042 and PSO001). This zone extends from a depth of around 24 km to 40 km and has a lateral extent of about 80 km. It is poorly resolved because of the strong local variation in the geoelectric strike of this region. However, it is not considered a spurious feature caused by localized 3-D responses in the data or 3-D structures at the southern end of the profile because it appears in both the joint and separate inversions of the individual modes and it is associated with a zone of lower apparent resistivity in the pseudosections (Fig. 7).

5.2. Lithospheric mantle resistivity model

Fig. 11 shows the resistivity model and data misfit for the lithospheric mantle. In this model the top 48 km, i.e., the crust, has been blanked out as the crustal data are in an inappropriate strike direction for the inversion. Data from a number of sites (ABIM06, ABI005, ABI006, PSO014, PSO022, PSO038, and PSO039) were excluded from the final sets of inversions because these sites exhibited high RMS misfit (>4) in earlier exploratory inversions. The global RMS error of the final model is 2.50. The misfit results show that it is possible to fit the TE mode data to a lower level of relative misfit than the TM mode data. The fit of the joint inversion model is found to be reasonably spatially uniform, except for some sites at the southern end of the profile. As shown by the pseudosection responses (Fig. 8), the large-scale features in the observed data are all replicated by the model response.

Fig. 11 shows that only the northwest and southeast ends, as well as the very deep parts of the lithospheric mantle, along the profile, are relatively conductive (<200 Ω·m). Beneath the CGB, there is a well resolved southeast-dipping highly resistive zone (labeled R in Fig. 11) that extends from the base of the crust to about 140 km depth. The upper part of the resistive feature is also visible in the crustal model beneath the CGB (Fig. 10). It extends laterally from the GF to the middle of the CMB. The resistivity of the feature is 2000–8000 Ω·m. The lithospheric resistor corresponds to a region of interpreted resistive and anisotropic rocks defined in earlier studies (Ji et al., 1996; Mareschal et al., 1995; Sénéchal et al., 1996). The resistor overlies a less resistive region, with resistivity of ~250 to 2000 Ω·m, that is still more resistive than adjacent parts of the lithosphere. This zone extends to a depth of around 280 km, and its southeastern extent is similar to that of the overlying more resistive zone.

The lithospheric resistivity model contains two isolated conductors. There is a conductor at approximately 80 km beneath the Pontiac Subprovince (labeled C2 in Fig. 11), and at the southern part of the

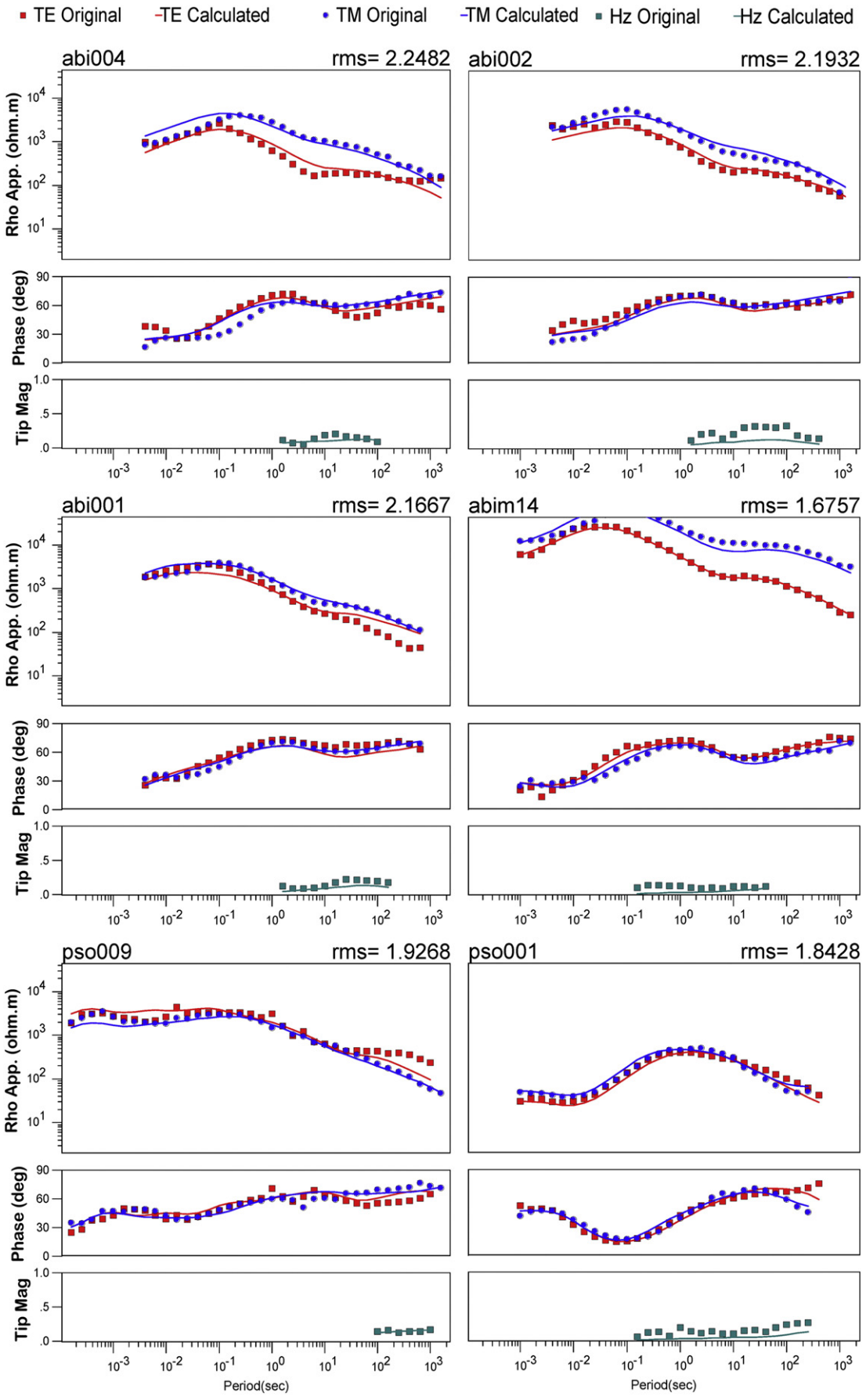
TE Original
TE Calculated
TM Original
TM Calculated
Hz Original
Hz Calculated
abi004
rms= 2.2482
abi002
rms= 2.1932
abi001
rms= 2.1667
abim14
rms= 1.6757
pso009
rms= 1.9268
pso001
rms= 1.8428
Rho App. (ohm.m)
Phase (deg)
Tip Mag
Period(sec)

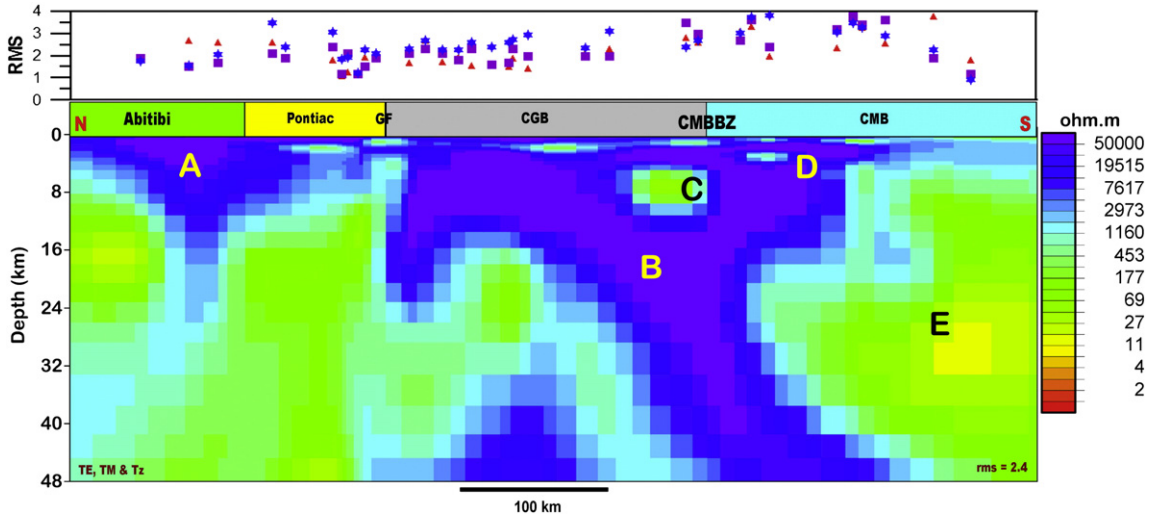

Fig. 10. 2-D resistivity section of the crust obtained by joint inversion of TE, TM and tipper responses for the crustal data set (V.E = 5). The RMS values of the TE (triangles), TM (stars) and joint TE + TM + Tz (squares) inversions at individual sites are plotted above the inversion model.

profile, a localized conductor (labeled C3) with conductivity between 10 and 20 Ω·m, is also resolved. This conductor lies between 100 and 150 km depth.

A prominent feature of the mantle lithosphere resistivity model is a deep conductor (labeled C1 in Fig. 11) beneath the southwest Superior Province. The top of the conductor is approximately horizontal and lies at a depth of about 150 km. Its resistivity is ~10 Ω·m. The conductivity of the feature increases beneath the Pontiac Subprovince (resistivity <5 Ω·m), where it is overlain by conductor C2. The form of the contour shown in Fig. 11 suggests that C2 is connected with a zone of enhanced conductivity within the horizontal part of conductor C1. Further to the southeast, the conductive feature appears to dip downwards beneath the Grenville Province but this part of the conductor is not properly resolved by the inversion and the apparent geometry is an artifact of the inversion.

Further data examination was carried out to confirm that the major resistivity structures in the final 2-D resistivity models are supported by the data. The key features in the model occur at depths at which the MT data from the overlying sites provide adequate penetration (shown in Fig. 3). Conductor C3 is primarily defined by the TE mode data, whereas resistor R and conductors C1and C2 are defined by the penetration of both TE and TM modes, as well as the Tz transfer functions. The conductors are associated with increase in phase or decrease in apparent resistivity at longer periods in the data. Conductors C2 and C3 can be related to conductive responses in the TE apparent resistivity response at periods of ~10^3 s. The northwestern part of Conductor C1 appeared in almost all of the various inversions, providing a reasonable fit to the long period MT data. The existence of the conductor is supported by the observation of high phase values (exceeding 70° in places) at periods >10^3 s in the TE and TM phase responses (Figs. 8 and 9). The absence of decreasing phase values at longer periods shows that the base of the conductor is not resolved, i.e., the electromagnetic fields at long periods do not penetrate through the conductor. The key features in the resistivity model are also imaged at sites where the data fit is good as shown in Fig. 11. Sites ABI001, ABI002 and ABI004 are directly above conductors C1 and C2, ABIM14 is above resistor R, while PSO001 is above conductor C2.

The necessity of the features in the resistivity model was examined by hypothesis testing using modeling and inversion. The joint inversion model was edited by removing the conductive and the resistive features (jointly and independently), and the resulting models were taken as starting models for a new series of inversions constrained to find the model closest to the starting model rather than the smoothest model, as is normally the case. The results consistently showed that conductors C1, C2 and C3, as well as the resistor R, are data-supported structures. The complete removal of conductors C1 and C2 or resistor R from the model consistently increased the global RMS misfit of the model by at least a factor of 3 and the RMS misfit of the individual sites also rose significantly. Although the resolution and shape of these features vary to some degree for different inversions, the results consistently suggest that the conductors and the resistor are first-order features existing in the subsurface.

6. Comparison of resistivity models with seismic results

6.1. Crustal model

Fig. 12 shows the location of the MT profile relative to seismic results available in the study area. The seismic results include a seismic refraction/wide-angle reflection profile that is approximately coincident with the southeastern part of the MT profile, as well as seismic reflection lines 12, 16, 16A, 15, 32, 33 and 71 that provide overlap coverage over much of the profile. Fig. 13 shows the seismic reflection and refraction models of the study area. Calvert and Ludden (1999) and White et al. (2000) used the Lithoprobe depth-migrated, near-vertical incidence, seismic reflection data along with seismic refraction-wide angle reflection velocity model to construct the cross-section of the crust in this region. The seismic profiles used include Lithoprobe lines 12 and 16 (Calvert and Ludden, 1999), line 16A (Benn et al., 1994), line 15 (Kellett et al., 1994), and lines 32 and 33 (White et al., 2000). Zhang and Frederiksen (2013) provide scattering tomography P and S velocity models for the crust in the study area but neither the P- nor S-velocity models show significant correlation with tectonic structures and the interpretation of their results remains uncertain.

Seismic reflection results show that the southern end of the Abitibi Subprovince is characterized by a half graben structure (Benn, 2006; Calvert and Ludden, 1999), and that the Pontiac crust is primarily

Fig. 9. Comparison of the observed and model TE and TM apparent resistivity and phases as well as the tipper responses at six sites along the MT profile. The results are for the inversion of the lithospheric mantle data set using the strike azimuth of 85°. The model response shown is obtained from TE + TM + Tz data and the RMS misfit for each site is shown above it. Sites ABI001, ABI002 and ABI004 are located in the Pontiac Subprovince, ABIM14 is located in the CGB, PSO009 is located on the CMBBZ and PSO001 is the southeasternmost site.

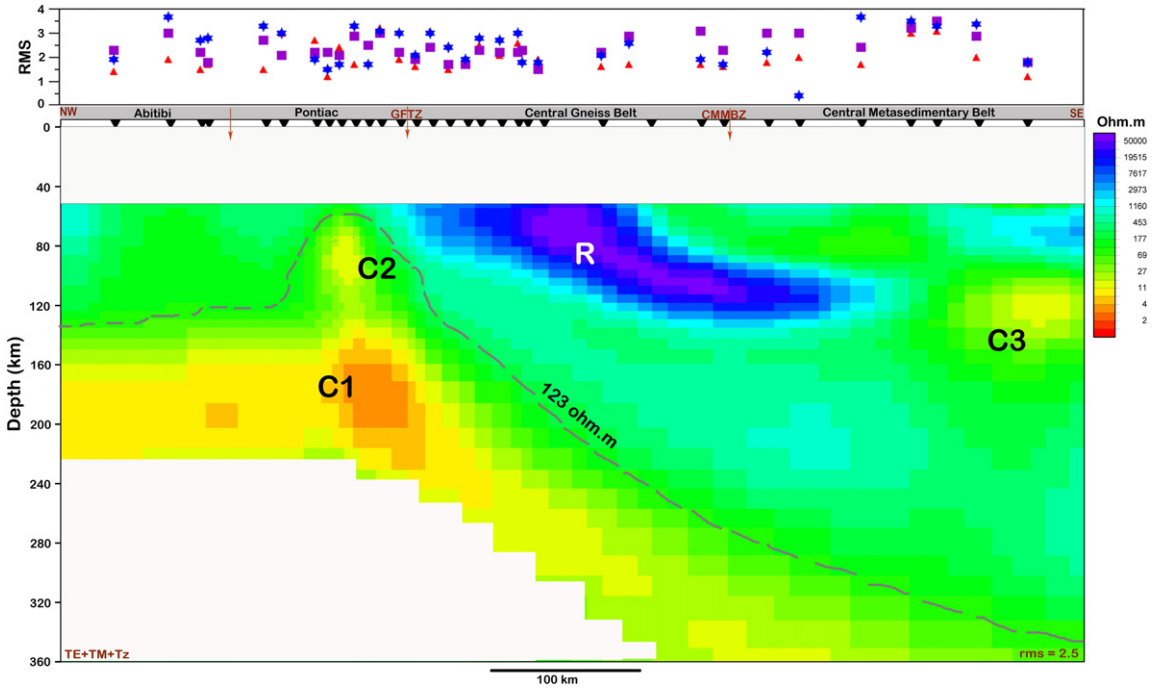

Fig. 11. Resistivity model derived by joint inversion of TE, TM and tipper responses for the lithospheric data set (V.E = 1). The RMS values of the TE (triangles), TM (stars) and joint TE + TM + Tz (squares) inversions at individual sites are plotted above the inversion model. The crustal section (upper 48 km) of the model is not shown. The lower section of the model in which there is no data resolution (below the lithospheric mantle conductor C1) has been blanked. The 123 Ω·m contour is shown in order to better define the depth extent of the more resistive part of the mantle.

made up of a mid-crustal duplex, underlain by a deeper thrust and overlain by near surface thrusts (Benn et al., 1994; Calvert and Ludden, 1999; Kellett et al., 1994). To the west of the study area, the GFTZ is 32 km wide (Green et al., 1989). Within the study area, it is a zone of southeast dipping stacked crustal sheets that extend to a maximum depth of 25–30 km (White et al., 2000).

The near-vertical and wide-angle seismic reflection data show dominantly southeast dipping reflectivity throughout the Grenville Province (White et al., 2000). The seismic results are interpreted to show southeast to northwest assembly of allochthonous crustal elements making up the CMB, followed by the deformation of this unit and its northwest transport over the rocks of the Laurentian margin (CGB) and pre-Grenvillian Laurentia (southeast Superior craton) (White et al., 2000). The reworked pre-Grenvillian Laurentia and Laurentian margin rocks are interpreted to extend at least 350 km south of the GF. Roy and Mereu (2000) showed that the CMBBZ is characterized by bands of southeast-dipping shallow reflectors extending to mid-crustal depth of 25 to 30 km. O'Dowd et al. (2004) defined this zone to be 10 to 12 km wide.

Fig. 14 overlays the seismic reflection image on the 2-D crustal resistivity model. The figure shows previous interpretations of the seismic reflection data (e.g., Benn et al., 1994; Calvert and Ludden, 1999; Kellett et al., 1994; White et al., 2000) (solid lines) and some modified interpretations (dashed lines) based on the combined resistivity and seismic reflection information. Within the Grenville Province, the strongest dipping reflectors are associated with very resistive regions in the resistivity model. There are prominent packages of reflectors, interpreted in previous studies (White et al., 2000) to correspond to the GF and CMBBZ, near the upper and lower surfaces of the dipping resistor (Feature B in Fig. 10). Strong coherent reflectors also occur within the resistive upper crust (Feature D) several tens of kilometers to the southeast of the CMBBZ. Further to the southeast, the reflectors associated with more conductive parts of the crust are more diffuse or sparse, and have irregular dips. There are no reflection data available in the area of the crustal conductors (Features C and E) in the Grenville Province.

6.2. Lithospheric mantle model

Fig. 12 shows the location of seismic tomographic images derived in studies by Rondenay et al. (2000) and Chen and Li (2012) and reproduced here in Figs. 15 and 16. Aktas and Eaton (2006) also conducted a tomographic study of the same region and Zhang and Frederiksen (2013) conducted scattering tomography.

In a large-scale teleseismic study, van der Lee and Nolet (1997) concluded that the Canadian Shied has a thick lithospheric root that extends to ~250 km depth beneath the Grenville Province. Smaller-scale seismic tomography studies have imaged a high velocity zone, or "seismic lid" in the upper lithosphere of the northern Grenville Province. It is defined in the Rondenay et al. (2000) (Fig. 15) and Chen and Li (2012) (Fig. 16) models as being between 50 and 100 km thick and lying between depths of 50 and 150 km. The strike direction of this anomaly is roughly parallel to the Grenville orogen tectonic trend (Aktas and Eaton, 2006; Chen and Li, 2012; Rondenay et al., 2000). Aktas and Eaton (2006) interpreted a high velocity anomaly within the Grenville Province as a relict slab associated with subduction beneath the CMB at 1.25 Ga.

There are several differences in how the body is imaged in different seismic studies. In the Rondenay et al. (2000) model, the high velocity zone is separated into two parts by the underlying low velocity anomaly, but in the Chen and Li (2012) model it is continuous across the area of the low velocity zone. Considering the superior depth resolution of the surface-wave based results of Chen and Li (2012), it appears that the break in the high velocity zone is likely an artifact of upward smearing of the low velocity anomaly. In contrast to the body wave studies of Aktas and Eaton (2006) and Rondenay et al. (2000), Chen and Li (2012) show that the high velocity zone extends to the south of the current study area and that the velocity anomaly becomes stronger near the Appalachian Front. Considering the superior lateral resolution of the travel time inversion, it appears possible that the Chen and Li (2012) model is connecting separate anomalies to the north and south of Lake Ontario.

The resistor R1 imaged in this study is closely spatially correlated with the high velocity anomaly. The upper and lower surfaces of the resistor are at similar depth to those of the velocity anomaly resolved in

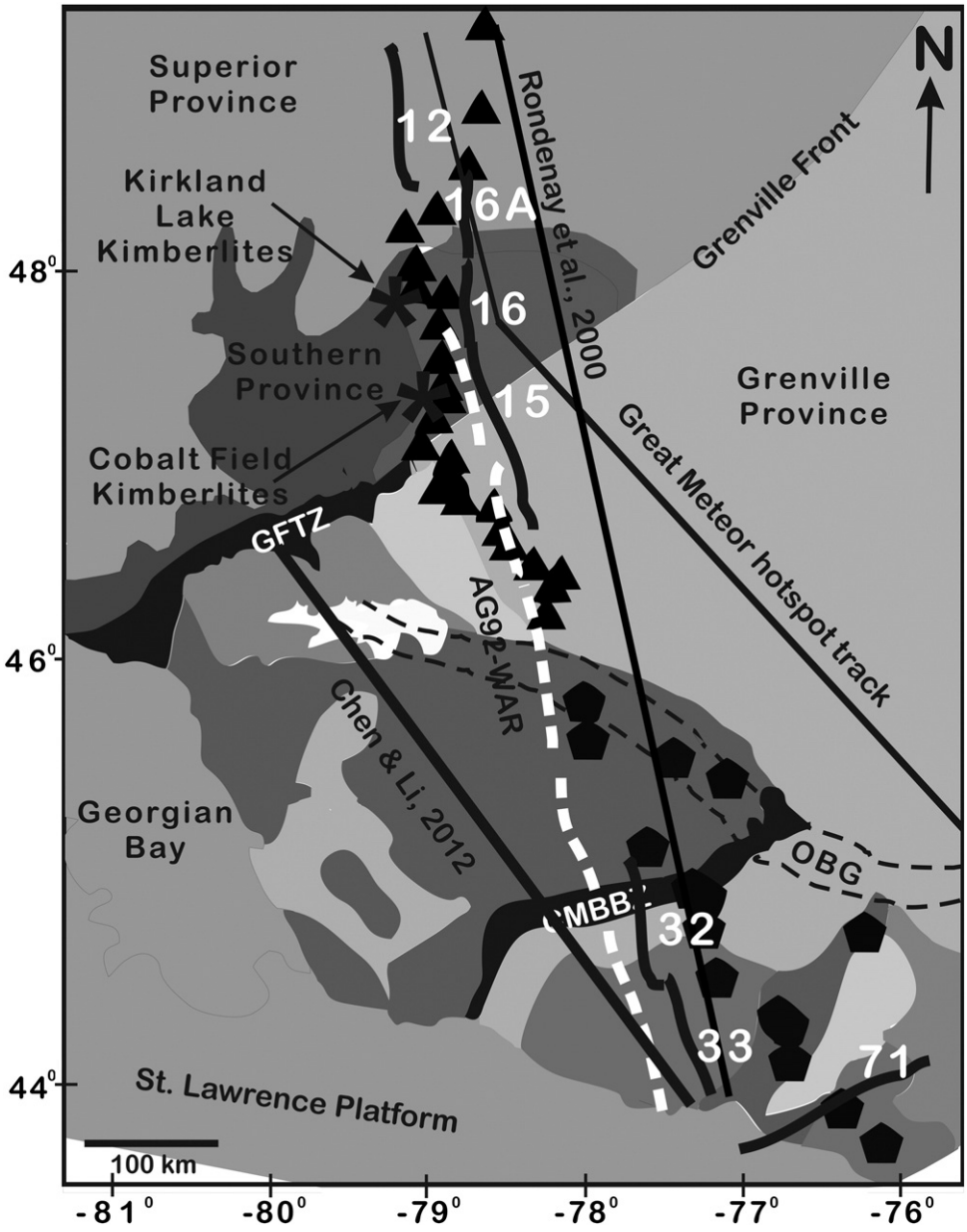

Fig. 12. Map of the study area showing the relationship between this study and previous seismic and tomography studies. The dashed white line indicates the Lithoprobe Abitibi–Grenville transect wide angle seismic refraction profile. Locations of Lithoprobe reflection seismic lines 12 and 16 (Calvert and Ludden, 1999), line 16A (Benn et al., 1994), line 15 (Kellett et al., 1994), and lines 32, 33 and 71 (White et al., 2000) are also shown. The black lines illustrate the Rondenay et al. (2000), Chen and Li (2012) seismic tomography studies as well as the surface track of Great meteor hotspot track defined by Crough (1981). The locations of the Kirkland Lake and Cobalt kimberlite fields are also indicated.

the surface wave study of Chen and Li (2012). The northern limit at 47° N is consistent with the northern limit of upper lithospheric (<150 km) high velocities in the Aktas and Eaton's (2006) and Rondenay et al.'s (2000) body-wave tomography models.

Taken together, the seismic and MT results provide compelling evidence for a coincident high-velocity, high-resistivity zone in the upper lithosphere extending southwards from near the Grenville Front. The southern limit of the feature is less well resolved but the MT and body wave seismic inversions suggest that a maximum southern extent is a point beneath the Frontenac terrane. Based on the resistivity model, the top of the body dips to the southeast from near the Moho at the GF to around 80 km depth beneath the Frontenac terrane. The base of the anomaly increases from around 80 km beneath the GF to around 150 km beneath the Frontenac terrane.

The seismic tomography also identifies a low velocity anomaly in the study area. Rondenay et al. (2000), in their P-wave travel-time inversion results (Fig. 15), resolve a near-vertical, WNW–ESE-trending low velocity anomaly. This anomaly extends between 50 and 300 km depth, with a relatively constant width of ~120 km. Aktas and Eaton (2006), also using body wave travel-time tomography, imaged the same anomaly and referred to it as a patchy NW-trending low velocity anomaly. Chen and Li (2012) produced a 3-D shear wave model of this region using a surface-wave two-plane wave inversion method, and their result (Fig. 16) shows a near-vertical anomaly similar to those imaged by earlier studies but in their model the top of the anomaly is at 150 km depth.

The low velocity anomaly is interpreted as being spatially correlated with the Great Meteor hotspot track by Aktas and Eaton (2006), Chen and Li (2012), Eaton and Frederiksen (2007), and Rondenay et al. (2000). The geometry and location of this anomaly approximately match an indentation in the North American lithospheric root defined by Fouch et al. (2000). This indentation is parallel to, and located to

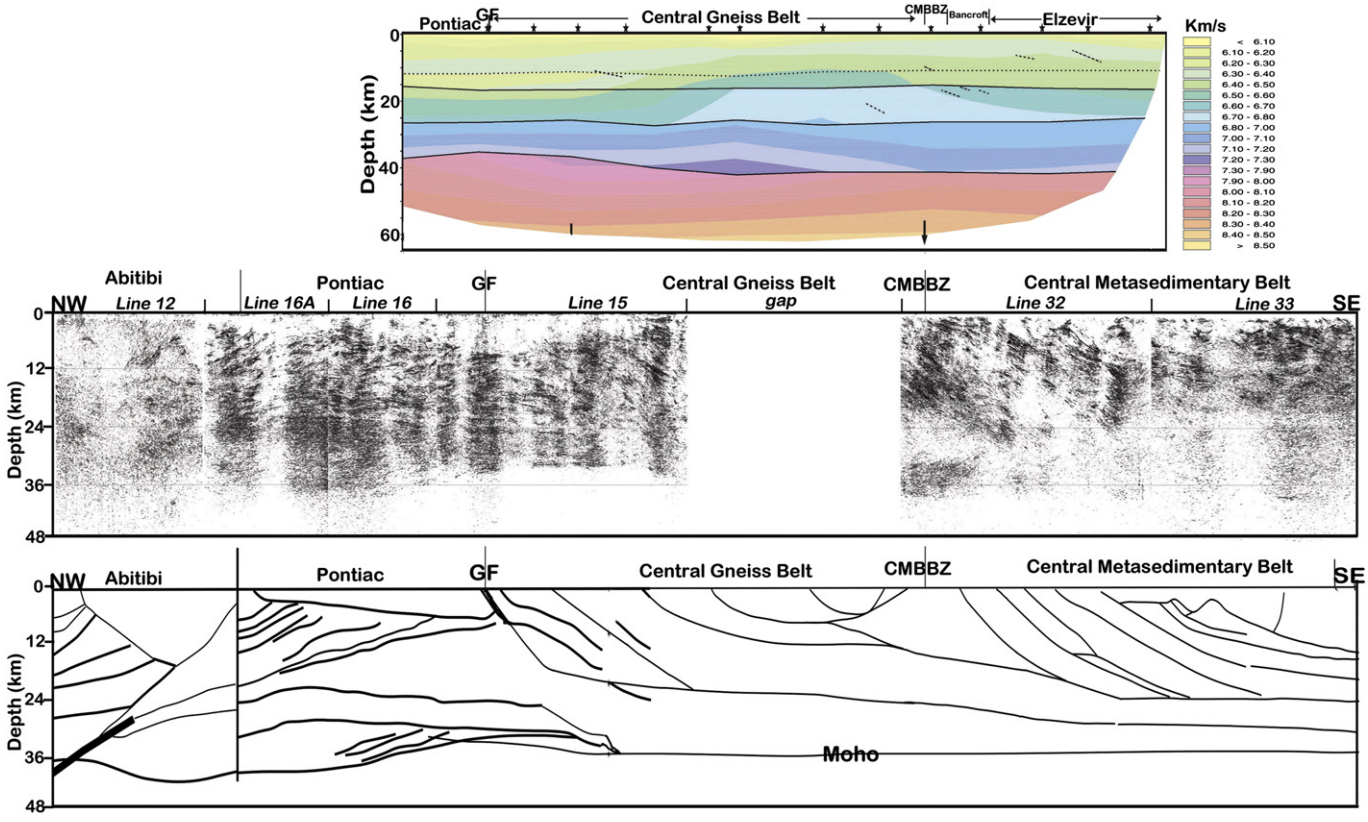

Fig. 13. Previous seismic reflection and refraction (wide-angle reflection) models of the study area. The seismic refraction wide-angle reflection model (top) is from White et al. (2000). The middle panel shows a composite seismic reflection image from Lithoprobe seismic reflection lines 12 and 16 (Calvert and Ludden, 1999), line 16A (Benn et al., 1994), line 15 (Kellett et al., 1994), and lines 32 and 33 (White et al., 2000) through the boundary zones. The bottom panel represents the crustal seismic interpretation from Ludden and Hynes (2000) and White et al. (2000).

the southwest of, the Ottawa Bonnechere Graben. Faure et al. (2011) interpreted this feature as a mantle scar, produced during Neoarchean subduction, which has been reused by several magmatic events.

The low velocity lithospheric anomaly imaged in the seismic tomography study lies to the south of the NW–SE dipping lithospheric conductor C1 imaged in this study (Fig. 15). The lateral position of the seismic anomaly is defined accurately in the body wave travel time tomography studies of Aktas and Eaton (2006), and Rondenay et al. (2000), both of which involved relatively high site density. Likewise, the lateral position will be quite well resolved in the MT 2-D inversions as it is defined by both the TE and TM mode data. Although the seismic low velocity and low resistivity anomalies have a somewhat similar geometry, they are clearly distinct features. The resistivity is relatively uniform and resistive in the vicinity of the seismic velocity anomaly. However, there is a weak low velocity response observed in the vicinity of the resistivity anomaly.

7. Interpretation and discussion of geoelectric strike

The geoelectric strike results show geographically consistent, but different, strike azimuths for the crust, lithosphere and the asthenosphere of the Grenville Province and adjacent Superior Province in southern Ontario. The defined crustal geoelectric strike (45°) is approximately parallel to the geologic strike of the GF and the CMBBZ in the study area. The strike azimuth for the crust exhibits more variability than the lithospheric and asthenospheric azimuths. These variations are attributed to some sites within the Pontiac Subprovince and the CMB. Within the CMB the variability is explained by the presence of

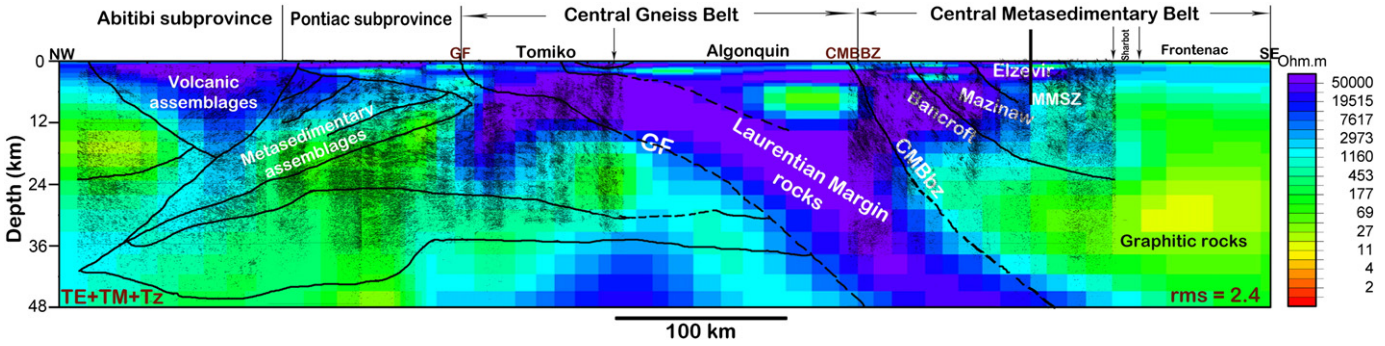

Fig. 14. The crustal resistivity model (V.E = 2.5) is overlain by seismic reflection profiles from Lithoprobe lines 12, 16, 16A, 15, 32, and 33. The Algonquin (in CGB), Sharbot and Frontenac (in CMB) terranes are not covered by the seismic studies. The black continuous lines show the interpretation of Kellett et al. (1994) for line 15, Benn et al. (1994) for line 16A, Calvert and Ludden (1999) for lines 12, and 16, as well as White et al. (2000) for lines 32 and 33. The dashed lines show the additions and modifications of the interpretation based on the resistivity data.

polyfolded domains with complex geometry and by the brittle to brittle–ductile thrust and normal faults that separate the domains (White et al., 2000). These rocks contrast with the largely flat-lying, amphibolite–granulite facies magmatic gneisses to the north in the CGB.

This study defined a regional lithospheric strike direction of N85°E, which agrees well with the N80°E defined by earlier studies (e.g., Mareschal et al., 1995). The new MT sites in the present study suggest that this strike azimuth extends some distance south into the Grenville province and therefore that there may be additional controls on the strike direction to the deformation in transcurrent shear zones in the mantle as suggested by Ji et al. (1996).

Deeper (>200 km depth) geoelectric strike azimuth, can be compared with estimates of absolute plate motion (APM) e.g., as done by Simpson (2001) (Figs. 5d, 6c). The APM direction at each of the MT sites was defined using three different APM models: the model of Larson et al. (1997), which is based on Global Positioning System (GPS) results, has a mean direction of 277°; the APM model of Demets et al. (1990), which is based on no-net-rotation reconstruction, has a direction of 279°; and the model of Gripp and Gordon (2002), which is a hotspot-referenced model, has a direction of 248°. The observed asthenospheric (>200 km depth) geoelectric strike azimuth is in excellent agreement with the Gripp and Gordon (2002) direction but it appears that this global APM model provides a poor estimate of the true plate motion in the study area. The Gripp and Gordon (2002) result, which is the estimate of the direction of the trace a hotspot would make over the last 50 Myr, is oblique to the interpreted surface trace of the Great Meteor hotspot for 150 to 115 Myr (Eaton and Frederiksen, 2007). The Great Meteor hotspot trail implies an approximately northwest plate motion in the study area, closer to direction indicated by the other APM models. Frederiksen et al. (2006) show that, the shear-wave fast direction, in the study area, coincides with the direction of plate motion defined by Larson et al. (1997).

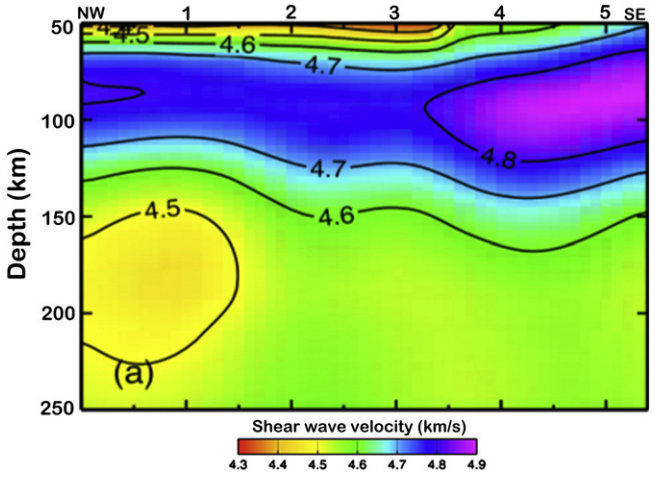

Fig. 16. Seismic surface-wave tomography model of Chen and Li (2012) for NW–SE profile through the present study area. See Fig. 12 for profile location: the present study area extends over the distance interval 0 to 3. The image shows the absolute S-wave velocity.

The results of the present study therefore indicate that the deep (>200 km) geoelectric strike is oblique to both the plate motion and seismic fast direction. Similar obliquity has been observed in other Precambrian cratons (e.g., Hamilton et al., 2006; Simpson, 2001). In the Grenville–Superior area, the observed obliquity provides support for interpreted lithospheric deformation in the region (Eaton and

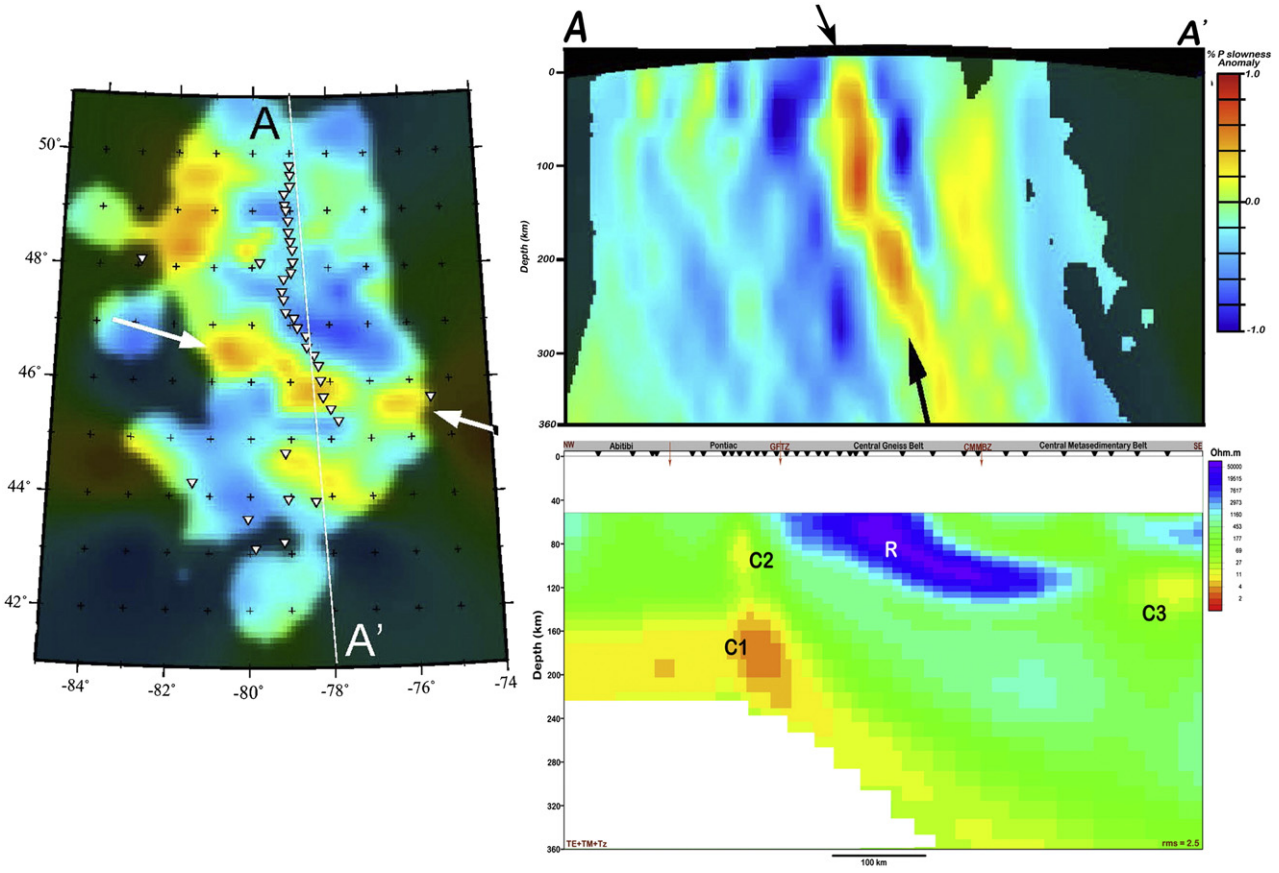

Fig. 15. Comparison of seismic body-wave tomography results of Rondenay et al. (2000) with resistivity model. Left panel shows the location of the seismic tomography profile and upper right panel shows the percentage P-wave slowness anomaly. Arrows define the low velocity zone. Lower right panel shows the lithospheric mantle resistivity model at the same horizontal and vertical scale as the seismic image.

Frederiksen, 2007). The deep geoelectric strike has the same sense as an observed offset between the surface trace of the Great Meteor hotspot and the seismic velocity "divot" observed at depths of 200 km that it is interpreted to be associated with the hotspot. The offset is explained by Eaton and Frederiksen (2007) by deformation of the lithospheric keel arising from viscous coupling with asthenospheric flow. Noting that the Niblett–Bostick depth transform used in the study is an approximate transform, and therefore that there may be some contribution to the "asthenospheric" results from lithospheric depths; the MT results are also consistent with such deep lithospheric deformation.

8. Interpretation of crustal resistivity structures

8.1. The Abitibi Subprovince

Fig. 14 shows the interpretation of the crustal resistivity model based on previous seismic reflection results and known surface geology of the region. Seismic reflection interpretations suggest that the crust of the Abitibi has a three-layer form (Benn, 2006; Calvert and Ludden, 1999). The upper to middle crust, at the northwestern end of the resistivity model, corresponding to the upper layer in seismic reflection models, includes a very resistive, synformal structure that extends to about 20 km depth. Our interpretation of the MT results follows the original interpretation of reflection seismic line 12 which suggests that this feature is a half graben developed as a result of large-scale extension (Calvert and Ludden, 1999). The surface geological evidence suggests that this feature consists of stacked volcanic assemblages of the southern volcanic zone of the Abitibi Subprovince (Ludden and Hubert, 1986). The high resistivity in the upper crust of the Abitibi may also be due locally to the granitic plutons intruded into what are now shallow depths (e.g., Benn, 2006).

The high resistivity of the Archean upper crust of the Abitibi Subprovince was noted in earlier MT studies. In Precambrian basement terranes, metasedimentary rocks, and particularly pelitic rocks, are observed to be more conductive than metavolcanic rocks or granites because of their increased content of conducting elements such as graphite or sulfides (e.g., Boerner et al., 2000; Ferguson et al., 1999; Korja et al., 2002). Deformation can further increase the conductivity by increasing the interconnection of these elements (Gowan et al., 2009; Jones et al., 1997).

Boerner et al. (2000) speculated that the lack of enhanced conductivity in the metasedimentary rocks of the southern Superior Province may be due to the limited extent, or poor preservation, of anoxic basin sediments. Earlier high resolution MT studies have shown mild enhancement of conductivity at regional scale fault zones in the Abitibi, such as the Destor-Porcupine deformation zone (Boerner et al., 2000; Zhang et al., 1995). However, this enhanced conductivity is not resolved by the subset of MT sites included in the present regional-scale study.

The middle crust of the southern Abitibi has different reflectivity patterns from the upper crust, and was interpreted by Calvert and Ludden (1999) to be of unknown affinity, with the upper crust representing an allochthonous unit. Benn (2006) re-interpreted the seismic reflection data and suggested that the middle crust consists of tonalite–trondhjemite–granodiorite (TTG) gneiss and paragneiss and that the upper crust and middle crust represent a single, differentiated autochthonous unit. The lower crust of the southern Abitibi is interpreted by both Calvert and Ludden (1999) and Benn (2006) to represent older, pre-3000 Ma crust from beneath the Pontiac Subprovince wedged into the Abitibi Subprovince (Fig. 14).

The resistivity model (Fig. 14) shows that the middle to lower crust of the Abitibi Subprovince is relatively conductive, and provides no differentiation between the lower two seismic zones. In earlier interpretations (Boerner et al., 2000 and references therein), the enhanced conductivity of the middle crust of Archean terranes of the southern Superior was thought to reflect the present-day state of the crust rather than inherent conductivity within the Precambrian rocks. This interpretation is re-examined below in light of the new results from further south in the Grenville Province.

8.2. The Pontiac Subprovince

The Pontiac Subprovince was imaged by seismic lines 16, 16A and part of 15. At the northern end of the Pontiac Subprovince, the interpreted seismic reflection packages dip to the north and extend beneath the surface boundary of the Abitibi Subprovince. Southward thinning fan-shaped packages of reflectors are interpreted to represent the expression of the Pontiac metasedimentary rocks at depth (Calvert and Ludden, 1999). In the same area the resistivity image shows a northwest dipping boundary between a more resistive zone and more conductive rocks at depth. The more conductive rocks are interpreted to correspond to the metasedimentary rocks, with the increase in conductivity with depth occurring as a result of thrusting. The geophysical results, along with the structural studies of Camire and Burg (1993) and Dimroth et al. (1982) which indicate the presence of south-verging folds in the Pontiac, suggest that the southern Abitibi overthrusts the Pontiac Subprovince.

The upper few kilometers of the Pontiac crust along much of the profile are relatively resistive. This is attributed to the presence of granitic rocks of the Décelles batholith that was intruded towards the end of the accretionary process. The southernmost 10 km of the subprovince is more conductive and correlates with a zone of metagraywacke and pink granite (Kellett et al., 1994). The enhanced conductivity is again attributed to the metasedimentary component of the rocks. As observed in the Abitibi Subprovince the middle and lower crusts in the Pontiac Subprovince are relatively conductive, as previously noted by Kellett et al. (1994).

8.3. The Grenville Front

At crustal scale, the observed resistivity structure in the region of the GF and the GFTZ consists of a southeast-dipping resistivity contrast extending from the upper crust to the base of the crust (Fig. 14). This contrast separates more conductive rocks to the northwest from very resistive rocks to the southeast. At 10 to 15 km depth, the resistivity contrast correlates spatially with very strong southeast-dipping reflectivity that is interpreted to represent the GF (e.g., Kellett et al., 1994; White et al., 2000). The correlation of the resistivity and seismic reflection results provides an indication that the GF is represented in the 2-D resistivity model by a boundary between more conductive Archean Pontiac rocks to the northwest and significantly more resistive rocks of the CGB to the southeast. Boerner et al. (2000), based on the earlier work of Kellett et al. (1994), interpreted the increase in resistivity to be associated with an increase in metamorphic grade across the GFTZ from the Archean foreland into the allochthonous rocks of the CGB.

Seismic profiles across different parts of the Grenville Province have indicated different depths of penetration for the GF (Martignole and Calvert, 1996; White et al., 2000). Ludden and Hynes (2000) interpret the penetration of the GF, as a normal fault, throughout the crust and into the mantle. The MT results from the present study provide confirmation that the GF extends to at least the base of the crust. The resistivity contrast can be traced clearly to this depth (Fig. 14). This interpretation is also consistent with that of the seismic reflection results by White et al. (2000) that suggest that the Archean footwall rocks are preserved along the length of the GF and extend a significant distance beneath the Grenville Province.

At upper-crustal scale, the 2-D resistivity model from this study supports the earlier interpretations that the GF has a relatively steep dip in the upper 6 to 8 km (e.g., Kellett et al., 1994). The resistivity model includes a prominent resistive block extending to around 20 km depth immediately beneath the GF. This feature is well resolved and appears in all inversion models. This part of the crust was interpreted by Kellett et al. (1994) to correspond to metagraywacke and orthogneiss.

However, based on the observation of significantly lower resistivity in the metagraywackes closer to the surface, the MT results suggest that the resistive unit may consist largely of orthogneiss.

The seismic interpretation of Culshaw et al. (1997) and Green et al. (1988) indicates that the GFTZ is the shear zone that penetrates the entire crust and propagates into the mantle. As noted by previous authors (e.g., Boerner et al., 2000) the resistivity models indicate that, unlike some other major fault zones elsewhere, the GFTZ is not characterized by a significantly enhanced conductivity. However, the result is consistent with observations at some other major Precambrian shear zones, e.g., the Great Slave Lake shear zone in northern Canada (Wu et al., 2002).

8.4. The Central Gneiss Belt

The 2-D crustal resistivity model shows that the CGB is characterized by a southeast-dipping package of highly resistive rocks that overly the GFTZ and extends to the lower crust beneath the CMB. These rocks have been interpreted as upper amphibolite facies, reworked, and displaced pre-Grenvillian Laurentia and Paleoproterozoic rocks (Rivers et al., 1989). The high resistivity can be attributed to the relatively low sedimentary component, the high metamorphic grade and the ductile thrusting the rocks underwent during the collisional process. Boerner et al. (2000) comment that the observed resistivity supports the surface geological mapping, by suggesting that there is no foreland basin type sediments preserved in the Archean foreland. However, more conductive rocks are observed at depth further to the southeast. The upper crustal conductive feature located in the CGB to the north of the CMBBZ lies within the Algonquin terrane. This anomaly is interpreted to correspond to a sequence of paragneissic rocks within this terrane. The enhanced conductivity is attributed to a component of graphitic or sulfidic metasedimentary rocks.

8.5. The Central Metasedimentary Belt Boundary Zone

In the 2-D resistivity model, the CMBBZ is interpreted to correspond to a strong resistivity contrast between the resistive rocks of the CGB to the northwest and more conductive rocks to the southeast. This feature is located immediately down dip of the seismic reflections and is oriented parallel to them, allowing it to be confidently reinterpreted in this study as the CMBBZ. The strong resistivity contrast can be traced from around 20 km depth to the base of the crust.

Based on this model, we interpret the CMBBZ as a southeast-dipping feature that extends throughout the crust and possibly propagates into the mantle, rather than rooting into a lower crust decollement as suggested by White et al. (2000). This reinterpretation means that accretion of the Laurentian margin rocks onto Laurentia, between 1080 and 1040 Ma, involved a whole crustal section rather than simple telescoping of the margin rocks onto older Laurentian crust. In this model, the lower crust of Laurentia is interpreted to extend only as far as to beneath the Elzevir terrane of the CMB rather than to further south beneath the Frontenac–Adirondack Belt, as suggested by White et al. (2000). The Sm–Nd data set also provides little evidence for Archean crust beneath the Frontenac–Adirondack Belt (e.g., Dickin, 2000). As with the GFTZ, the CMBBZ is characterized by an absence of enhanced conductivity, an observation which is consistent with the high metamorphic grade and ductile deformation that characterize the zone.

8.6. The Central Metasedimentary Belt

The resistivity model of the upper crust in the CMB includes very resistive rocks in the Bancroft terrane and northern part of the Elzevir terrane, and relatively conductive rocks in the southern part of the Elzevir terrane, the Sharbot Lake terrane and in the Frontenac–Adirondack terrane to the south. In seismic reflection lines 32 and 33, the zone of high resistivity in the upper crust is characterized by strong south-dipping reflectivity, whereas the more conductive area to the south is characterized by horizontal or irregular reflections.

The southeast margin of the resistive upper crust lies in the Elzevir terrane, and is interpreted to correspond to the transition between the Belmont domain to the north and the Grimsthorpe domain to the south. The higher conductivity in the Grimsthorpe domain can be attributed to the presence of volcaniclastic sedimentary rocks in that domain and also to the lower grade of metamorphism. The Belmont domain has been metamorphosed to amphibolite facies, whereas the Grimsthorpe domain records mainly greenschist facies metamorphism. Carr et al. (2000) note that the nature of the Belmont–Grimsthorpe boundary remains uncertain. The resistivity model from the present study suggests a near-vertical boundary between these units.

The relatively conductive upper crust in the Frontenac terrane can be attributed to an increased proportion of graphite or sulfides in the predominantly supercrustal rocks which include quartzofeldspathic gneiss, marble, and quartzite (Carr et al., 2000). The boundary between the rocks of the Composite Arc Belt and the Frontenac–Adirondack Belt is interpreted to be a south-dipping shear zone (Robertson Lake shear zone) extending into a regional mid-crustal decollement (Carr et al., 2000; White et al., 2000). The resistivity model provides no resolution of either enhanced conductivity or a resistivity contrast across this feature.

8.7. The middle and lower crustal resistivity

A number of MT studies in the southern Superior craton have mapped relatively conductive middle and lower crusts. The enhanced conductivity has been observed to cross major structural boundaries, e.g., between the Abitibi and Pontiac subprovinces (Sénéchal et al., 1996), between the Abitibi and Kapuskasing structural zone (Kurtz et al., 1993), and between the Pontiac Subprovince and the northernmost Grenville terrane (Kellett et al., 1994). In the Kapuskasing structural zone, enhanced conductivity cuts across steeply-dipping structural and seismic reflection fabric (Boerner et al., 2000). These observations led to the interpretation that the enhanced conductivity reflects the present day mechanical and fluid state of the crust rather than an inherent feature of the Precambrian rocks that are present (Boerner et al., 2000; Mareschal et al., 1995). Boerner et al. (2000) noted that for the Abitibi–Grenville region, the interpretation is based only on observations from the Superior and northernmost Grenville crust.

As discussed above, the results from the current study define a well-resolved resistive zone, corresponding to the rocks of the CGB, extending into the lower crust. They also define a localized zone of enhanced conductivity beneath the Frontenac terrane. The dipping nature of the resistive rocks of the CGB, and the localized extent of the Frontenac conductor indicate control on resistivity by the associated Precambrian rocks. This observation suggests a significant difference in controls on middle and lower crustal resistivity in the Grenville and Superior Provinces.

Boerner et al. (2000) discuss the constraints on the timing of the formation of the conductive middle and lower crusts in the southern Superior. Evidence for widespread tectonic activity in the deep crust of the Superior Province includes 2660–2580 Ma growth of metamorphic zircon and 2520–2400 Ma overgrowths on Archean zircons in kimberlite xenoliths. However, these events predate the formation of the ~1900 Ma Kapuskasing Structural Zone in the Paleoproterozoic in response to the Hudsonian orogeny (Kerrich and Ludden, 2000) and cannot explain the continuity of enhanced conductivity across the boundaries of this structure. Fluid events at 1950–1800 Ma associated with the actual formation of the Kapuskasing Structural Zone (Kerrich and Ludden, 2000) provide a more suitable timing provided that a component of the fluid flux occurred late in the tectonic process.

The rocks in the dipping resistor created by the CGB are of Archean to Mesoproterozoic age. The bounding faults of the structure, the CMBBZ and the GF, were active at around 1080–1060 Ma and ca. 1000 Ma respectively (Carr et al., 2000). Late normal faulting on these shear zones may be as young as 850 Ma (Ludden and Hynes, 2000).

The observation of structures of this age cutting across the conductive lower crust implies that the pervasive enhanced mid-crustal conductivity to the northwest is either older than these dates or, if it is younger, it occurs in a restricted geographical area. The observations would appear to exclude the suggestion by Mareschal et al. (1995) that the enhanced conductivity is associated with a present-day ductile lower crust.

The lower crustal conductor that exists in the Frontenac domain is not well resolved in the crustal model. The feature is however consistently present in all crustal models and also appears well-resolved in the lithospheric model (Fig. 11). Along with the poorer fits to the GB decompositions for the CMB, the result suggests that the conductive feature may have a strike that lies closer to east–west than the 45° azimuth used in the 2-D inversions of the crustal data set.

Enhanced electrical conductivity in the lower continental crust is usually interpreted to be caused by fluids, graphite, and/or sulfide-bearing rocks of sedimentary sequences that have undergone complex deformation such as thrusting (Jones, 1992; Korja et al., 1996; Schwarz, 1990). The localized geometry of the conductive zone would be very difficult to explain in terms of a fluid source. The Frontenac terrane consists of a succession of multiply deformed, relatively low-pressure, granulite facies, quartzofeldspathic and pelitic gneiss, quartzite and marble intruded by plutonic rocks and subjected to metamorphism (Easton and Davidson, 1997). Easton (1992) suggested that the Frontenac terrane is different from other terranes within the CMB in terms of composition (it lacks volcanic rocks) and in that in it is preserved granulite facies rocks in contrast to the lower grade facies to its north (Bancroft and Elzevir) and south (Adirondack lowlands). The hypothetical stratigraphy of this terrane consists of two stacked sets of tripartite units composed from bottom to top, gneiss, quartzite and marble (Hildebrand and Easton, 1995). The marble in the Frontenac terrane is composed of calcite with varying proportions of graphite, serpentine and calc-silicate minerals (Hildebrand and Easton, 1995). The lower conductor is thus fairly reliably interpreted to be caused by graphitic rocks of the CMB.

9. Interpretation and discussion of lithospheric mantle resistivity structure

9.1. High-resistivity zone beneath the northwest Grenville Province

Fig. 17 shows the 2-D resistivity model of the study area along with our interpretation of the prominent features. An important feature of the lithospheric resistivity model is the southeast-dipping resistive feature that extends from ~40 to 140 km depth. This northwest-striking resistivity anomaly extends laterally from GF into the middle of the CMB at depth and includes resistivity values exceeding 2000 Ω·m. As described above there is excellent spatial correlation of the high resistivity anomaly with a seismic high velocity anomaly.

Two explanations for the seismic high velocity zone have been proposed: that it is either associated with depletion of iron in the cratonic lithosphere (Chen and Li, 2012) and/or that it is a relict slab associated with the Early Proterozoic subduction beneath the CMB (Aktas and Eaton, 2006). The high velocity observed in the feature can be explained petrologically by either an increased Mg to Fe ratio in a peridotitic or harzburgitic mantle, or to the presence of eclogite and garnet phases produced by plate subduction (Chen and Li, 2012).

An increased Mg to Fe ratio, for example associated with depletion of the mantle, would also be associated with increased electrical resistivity (e.g., Fullea et al., 2011; Jones et al., 2009a; Selway, 2013). Petrological studies of mantle xenoliths from different parts of the world have confirmed the existence of systematic variations in the composition of the lithospheric mantle due to depletion of the cratonic mantle in basaltic components, primarily iron, aluminum and volatiles, which results in the increase of the upper mantle resistivity (Artemieva, 2009). The first explanation for the high velocity is therefore in accord with the resistivity results.

The second explanation of the high velocity is less compatible with the MT results in this study as the resistivity model differs significantly from models commonly observed in plate subduction settings. In regions of active subduction, resistivity anomalies are dominated by enhanced conductivity rather than dipping resistors (e.g., Jödicke et al., 2006; Soyer and Unsworth, 2006). The enhanced conductivity, which may form localized features, is interpreted to be caused by fluids released by the subducting slab. The resulting anomalies have been observed to persist for a long duration following the cessation of subduction (e.g., Ledo et al., 2004) and it is generally expected that refertilization of the mantle by the fluids will lead to long-lived enhanced conductivity (Selway, 2013). The relatively conductive uppermost mantle lithosphere observed downdip from the southeastern CGB and CMB in Fig. 11 could be interpreted as enhanced conductivity associated with subduction, but the thick resistive slab represents an unusual observation in a subduction setting.

The mantle lithosphere beneath the northern Grenville Province may have formed by one of two mechanisms. If the lithosphere is in situ and the same age as the overlying upper crustal rocks, it must have developed during the series of long-lived orogenies that accreted

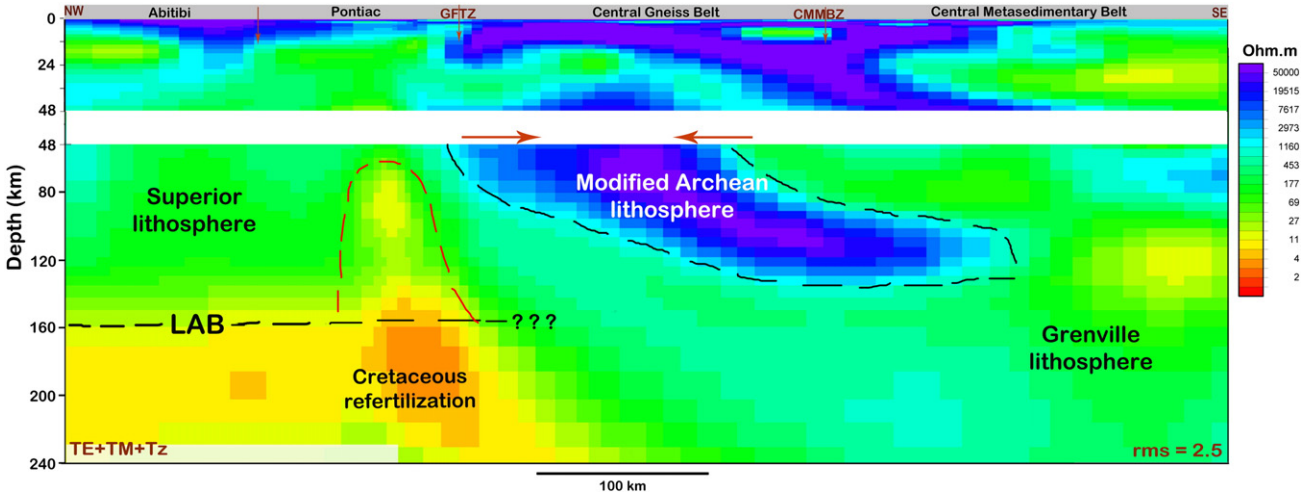

Fig. 17. Interpretation of features in lithospheric mantle resistivity model. The figure shows the 2-D lithospheric resistivity model (V.E = 1), interpretation of the resistive block in the shallow mantle lithosphere as being modified Archean lithosphere, interpretation of the conductive zone at 160 km depth as the LAB beneath the southeastern Superior province, and interpretation of a localized conductor as a lithospheric mantle scar refertilized in the Cretaceous by passage of the Great Meteor hotspot. The correct model (for the strike azimuth appropriate at crustal signal penetration) is shown above the lithospheric model. The arrows show the part of the model used to define the averaged resistivity profile shown in Fig. 18.

Andean arc and back arc rocks onto the Laurentian margin between 1.9 and 1.2 Ga. However, there is strong evidence to suggest that the accretion of the Proterozoic rocks before and during the Grenville orogen occurred onto Archean basement of the Superior Province. The observation in both seismic reflection images and electrical resistivity images (this study) of the Laurentian margin rocks extending some distance to the south in the middle and lower crusts provides support for this interpretation. In other studies, Ludden and Hynes (2000) suggest that an Archean lithospheric root was responsible for providing a stable, cold, and relatively low density basement to the Grenvillian orogen. Hynes and Rivers (2010) inferred that the central Grenville Province is underlain at depth by Archean rocks of the Superior Province. Finally, within the study area there is no major change in the shear wave velocity at 150 km depth at the location of the surface margin of the Superior and Grenville Provinces (Faure et al., 2011) providing further support for the fact that the Grenville Province is underlain by the Archean mantle of the Superior Province.

The values of resistivity observed in the resistor beneath the northern Grenville Province are extremely high. Comparison of the Grenville results with a deep 2-D resistivity model crossing Proterozoic and Archean blocks in southern Africa (Muller et al., 2009) shows that in terms of the resistivity values, the upper 100 km in the Grenville lies between that observed in the East and West Kimberley blocks of the Archean Kaapvaal Craton and is approximately an order of magnitude more resistive than the lithosphere in adjacent Proterozoic terranes, including the Ghanzi-Chobe and Damara belts (Fig. 18).

The MT results do not provide definitive support for either of the proposed mechanisms of formation of the high velocity-high resistivity zone. The geometry of the high resistivity feature in the MT model includes a well-resolved dip to both the upper and lower surfaces, as would be expected for an anomaly related to a relict slab feature. The results also show that the base of the feature is relatively well defined

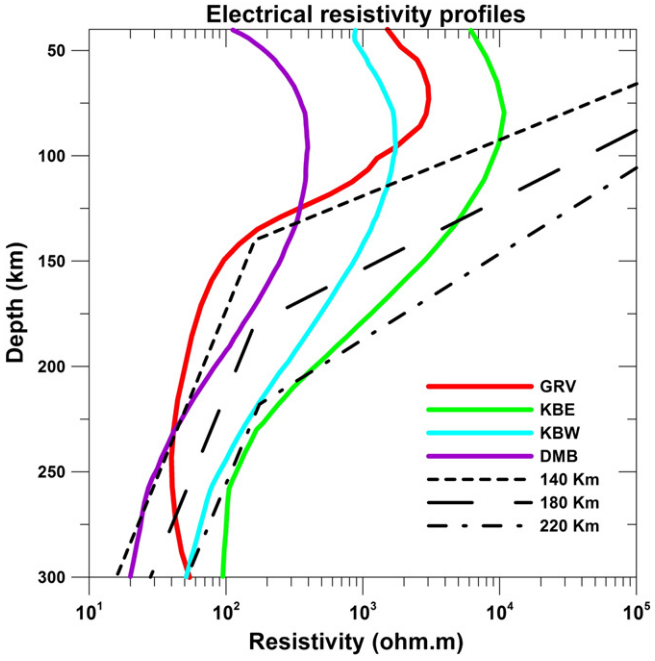

Fig. 18. Comparison of electrical resistivity depth profiles for the northern Grenville Province (GRV; this study), with the profiles for the Ghanzi-Chobe/Damara Block (DMB), Western Kimberley Block (KBW), and Eastern Kimberley Block (KBE; Muller et al., 2009). The average profile for the Grenville Province is computed for the area shown in Fig. 17. The theoretical resistivity-depth profiles calculated by Muller et al. (2009) for mantle geotherms of different lithospheric thicknesses are also shown in black. The laboratory measurements of the electrical-conductivity against pressure and temperature for dry olivine and pyroxene are used to compute the profiles (Constable et al., 1992; Xu and Shankland, 1999; Xu et al., 2000). The points of inflection on these curves coincide with the intersection between the adiabat and the conductive mantle geotherm (Muller et al., 2009).

(Fig. 18). However, as discussed above, it is presently unclear how a relict slab could create such highly resistive features, especially in the absence of any associated conductive anomalies. In addition, if this feature were to be a relict slab, it should be located down dip from the CMB or further southeast. In contrast to the geometry of the high resistivity zone, the actual values of resistivity observed provide support for formation of the feature by high levels of mantle depletion.

9.2. Deep, laterally-extensive, horizontal conductive anomaly

An important feature of the 2-D lithospheric resistivity model is the lithospheric conductor (C1) that extends horizontally beneath the southern Superior Province. The top of this feature is observed at around 160 km depth (Fig. 17).

A common interpretation for deep (>150 km) laterally-continuous conductors is that they represent the electrical signature of the lithosphere–asthenosphere boundary (eLAB) (Jones et al., 2010). The LAB depth has been estimated from a sharp change in mantle conductivity that is interpreted to be associated with the onset of partial melt (Artemieva, 2009; Jones et al., 2010) or of enhanced bound water in olivine and pyroxenes (Karato, 1990, 2012). Muller et al. (2009) describe an alternative method for estimating the LAB using comparison of resistivity-depth profiles derived for predicted geotherms with observed resistivity-depth profiles. This approach assumes a dominant thermal control on resistivity.

Fischer et al. (2010), using shear wave velocity, suggested that the seismically-defined LAB depth of the Superior Province ranges from 150 to 220 km. Darbyshire et al. (2007) suggested that the lithospheric thickness of the Superior Province in the study area varies from 100 to 220 km. Within the study area the estimated depth of the petrologic LAB beneath the southern Superior Province has been estimated using kimberlites from Cobalt and Kirkland Lake, to be 160 km (Griffin et al., 2004) and 144 to 150 km (Snyder and Grütter, 2010).

We interpret the horizontal portion of the lithospheric conductor in the southern Superior Province to be the eLAB. Our suggestion is supported by the success of electrical LAB depth interpretations elsewhere (Jones et al., 2010) and by the good agreement between the depth of 160 km indicated by the resistivity results and the seismic and petrological results for the southern Superior area. Fig. 18 shows theoretical resistivity profiles calculated by Muller et al. (2009) based on thermal models for different thicknesses of the lithosphere. For all models, the LAB coincides with resistivity values of 100 to 150 Ω·m. As shown in Fig. 11, this value of resistivity is attained at a depth of about 140 km beneath the southeastern part of the Superior craton. As noted in previous studies, the LAB depth is relatively shallow for an Archean craton. Faure et al. (2011) also show that the lithospheric seismic velocity at 150 km depth beneath the southern Superior craton is significantly less than farther to the north in the craton. These results have been attributed to the extensive tectonic processes that have affected this region following formation of the craton, e.g., during the 2.4 Ga events associated with formation of the Huronian basin and the 1.8 Ga events associated with the Hudson orogen. In addition, the earlier postulated mantle plumes (Faure et al., 2011) and lithospheric subduction-dominated processes, associated with the formation of the Abitibi Greenstone Belt during the Neoarchean, may have modified the lithospheric mantle in this area (Daigneault et al., 2004).

9.3. Deep, subvertical conductivity anomaly

Another important feature of the lithospheric 2-D resistivity model is the subvertical conductor C2 beneath the Pontiac Subprovince. This conductor overlies enhanced conductivity at the depth of the interpreted LAB (Fig. 17).

Previous studies have concluded that the seismic low-velocity anomaly, farther to the south in the lithospheric mantle of this region, was formed as a result of the geochemical alteration of the mantle due

to the passage of the Cretaceous Great Meteor hotspot, which is the last tectonothermal event that affected this region (Aktas and Eaton, 2006; Chen and Li, 2012; Eaton and Frederiksen, 2007; Rondenay et al., 2000; van der Lee and Nolet, 1997). The alkaline volcanism of the Great Meteor hotspot is responsible for the emplacement of features along the Monteregian–White Mountain–New England seamount track (Crough, 1981). Faure et al. (2011) however suggested that the low velocity zone is produced by tectonothermal events (Early Proterozoic to Cretaceous) that have reused the permanent mantle scar left by the early modification of the mantle during the formation of greenstone belts in the Neoarchean. This zone correlates spatially with the Neoarchean Greenstone Belt of the Abitibi Subprovince and its plume-driven subduction zone. Rondenay et al. (2000) and Faure et al. (2011) relate the low velocity anomaly to the magmatism responsible for the emplacement of the Kirkland Lake and Cobalt (Rapide des Quinze) kimberlite fields.

Selway (2013) reviewed sources of enhanced conductivity in tectonically stable lithosphere. She suggested that the electrical conductivity of stable lithosphere is mainly affected by hydrogen content of nominally anhydrous mantle minerals and grain boundary graphite films. A subduction or plume event may have introduced hydrogen and carbon into Archean lithosphere as much as several billion years ago and, if no high temperature events have occurred to remove those species, they will still remain to produce a conductive anomaly (Selway, 2013). However, it should be noted that not all regions of the mantle lithosphere in which metasomatism has occurred have decreased resistivity (Jones et al., 2002).

Considering both the controls on mantle resistivity and the results of the earlier seismic studies we interpret the enhanced conductivity in the sub-vertical conductor to have resulted from the re-fertilization of the mantle scar, initially created by an early thermomechanical event responsible for the formation of the Abitibi Greenstone Belt, by the Cretaceous Great Meteor hotspot plume. We propose that the alkaline rich mantle plume, associated with the Great Meteor hotspot, refertilized the mantle by re-introducing grain-boundary graphite films and possibly other incompatible elements by intrusion of melt through a weak zone within the lithosphere, thereby increasing the conductivity of the zone. Following this interpretation, it is concluded that the conductivity structure is of Cretaceous age. Faure et al. (2011) pointed out that plumes that accumulate around the LAB interface form unstable pockets that migrate by excess pressure vertically through sub-vertical zones of weakness. This description is consistent with the observation of enhanced conductivity at the LAB beneath the subvertical conductor and indicates the existence of a complex interaction between the postulated mantle plume and the base of the lithosphere. This interaction is generally controlled by the geometry of the LAB or the lithospheric zones of weakness.

It is of note that the Mesozoic Kirkland Lake and Cobalt kimberlite fields are located about 50 km along strike from the lithospheric conductor (C2). It is therefore possible that diamondiferous kimberlites passed through the part of the region of lithosphere containing the subvertical conductor. The conductor itself lies above the diamond-graphite stability field at 140–150 km depth and may therefore be caused by graphite. However, the enhanced conductivity at the LAB lies within the diamond stability field and must therefore be explained in terms of mantle enrichment by other elements.

Jones et al. (2001) imaged a conductor beneath the Slave Craton in northern Canada, the Central Slave Mantle Conductor (CSMC). As observed in the present study, the conductor seems confined to depths of less than 130 km. The CSMC is collocated with an Eocene-aged kimberlite field in the Slave Craton. In earlier interpretations, the CSMC was interpreted to be due to carbon, either as grain boundary film or as graphite or water associated with subduction beneath the Slave craton (Jones et al., 2003). However, in a recent re-interpretation by Selway (2013), the enhanced conductivity is attributed to initial re-fertilization of the lithosphere by subduction and subsequent remobilization of the conducting constituents due to kimberlite emplacement (Selway, 2013). It is possible that such an interpretation also applies in the southern Superior, with the initial introduction of carbon and water into the mantle having occurred in the Archean and/or Proterozoic events with the remobilization occurring in the Cretaceous. In this case, the enhanced conductivity and decreased velocity observed beneath 160 km depth in this region may be attributed to the presence of refertilized lithosphere rather than to asthenosphere.

10. Conclusions

The MT data, collected at sites in southern Ontario, during the Lithoprobe-Abitibi Grenville Transect and POLARIS project, are used to image the Proterozoic Grenville Province and its margin with the Archean Superior Province.

The strike results show a different geoelectric strike azimuth for the crust, lithosphere and the asthenosphere of this region. The crustal geoelectric strike (45°) is subparallel to the surface geologic strike of the Grenville Front and the CMBBZ. The lithospheric mantle strike direction of N85°E agrees well with the N80°E defined by earlier studies, and the new observations extend the region of this strike direction farther south into the Grenville province.

A 2-D resistivity model determined using the crustal strike azimuth delineates a number of crustal structures. The upper crust of the Abitibi Subprovince is resistive and the middle to lower crust is relatively conductive. The upper crust in the Pontiac Subprovince contains some areas of increased conductivity that are attributed to the metasedimentary component of the rocks in the area. The new MT results, from farther south in the Grenville Province, provide confirmation that the GF extends to at least the base of the crust. Based on the resistivity model, the CMBBZ is interpreted as a southeast-dipping feature that extends throughout the crust rather than rooting into a lower crust decollement as suggested by White et al. (2000). Graphite-bearing rocks of the CMB are suggested to be responsible for the lower crustal conductor imaged beneath the Frontenac terrane.

The crustal resistivity model includes very resistive Laurentian margin rocks dipping southeast to the base of the crust, bounded to the northwest by the GF, and to the southeast by the CMBBZ. The observation is in contrast to the observation elsewhere in the region of conductive mid to lower crust and requires revision of the interpretation that the enhanced conductivity reflects present day geodynamic conditions. If a single event caused the enhanced conductivity, it must be younger than the 1950–1800 Ma formation of the Kapuskasing Structural Zone which is crosscut by the enhanced conductivity, and older than the 1080–1060 Ma age of the CMBBZ and the ca. 1000 Ma age of the GF which crosscut the enhanced conductivity. The Superior Province crust records a 1950–1800 Ma fluid event associated with the formation of the Kapuskasing Structural Zone which may explain the observations as long as a component of the fluid flux postdates the main deformation.

A 2-D resistivity model for the lithospheric mantle was derived using the corresponding strike azimuth. It defines a very resistive lithospheric layer that extends between approximately 40 and 140 km vertically and laterally from the GF southeast into the middle of the CMB. The feature corresponds to a high velocity zone in seismic tomographic models. The resistivity of this feature is comparable to that observed in depleted Archean lithosphere in southern Africa and suggests that the lithosphere has not been re-fertilized by young tectonic process (e.g., Selway, 2013). The geometry of the body suggests that it may be a relict slab of Superior craton lithosphere. As noted by previous authors, the presence of modified Archean lithosphere beneath the Grenville Province would have provided the necessary basement for the Grenvillian orogeny.

A lithospheric conductor that extends horizontally beneath the southern Superior Province with its top at 160 km is interpreted to represent the eLAB beneath that craton. The observed depth of the feature is in agreement with seismic and petrological information for the area. A sub-vertical conductor observed in the lithospheric mantle beneath the

Pontiac Subprovince overlies a region of enhanced conductivity at about 150 km depth. This feature lies well to the north of a sub-vertical low seismic velocity zone delineated in seismic tomography studies. We interpret the enhanced conductivity in the sub-vertical conductor to have resulted from re-fertilization of the mantle scar, initially created by an early thermomechanical event responsible for the formation of the Abitibi Greenstone Belt, by the Cretaceous Great Meteor hotspot plume. The location of the sub-vertical lithospheric conductor, which is along strike with the Kirkland Lake and Cobalt field kimberlite fields, also drives us to suggest that the diamondiferous kimberlites being produced in these fields passed through this part of the lithosphere. The assertion that MT is capable of imaging such enrichment is important for the interpretation of lithospheric structure and evolution. More importantly, the ability of MT to image such regions is useful for diamond exploration, as espoused by Jones and Craven (2004) and Jones et al. (2009b).

Acknowledgments

The authors thank the POLARIS southern Ontario MT team (J. Wenham, M. Serzu, X. Ma, E. Gowan, H. Sealey, T. Pacha, J. McCutcheon, B. Eade, I. Asudeh, C. Andrews) for MT data collection and landowners in the region for site access. Comments from A. Frederiksen, A. Camacho, A. Rajapakse, and two anonymous reviewers have led to significant improvement of the manuscript. The current study could not have taken place without M. Mareschal's important earlier work on the Abitibi–Grenville LITHOPROBE MT data. Funding for POLARIS has been provided by industry, the Canada Foundation for Innovation, provincial agencies from Ontario and British Columbia, the Federal Economic Development Initiative for Northern Ontario, Natural Resources Canada, and NSERC (Natural Sciences and Engineering Research Council of Canada). The present research was supported by an NSERC Discovery Grant (105748) to Ian Ferguson.

References

Adetunji, A.Q., 2013. The Resistivity Structure of the Grenville Province. (Ph.D. Thesis) University of Manitoba, Winnipeg, Canada.
Adetunji, A.Q., Ferguson, I.J., Jones, A.G., 2013n. Imaging the mantle lithosphere of the Grenville Province: large-scale structures and electrical anisotropy. Geophys. J. Int. (in preparation, Nov.).
Agarwal, A.K., Poll, H.E., Weaver, J.T., 1993. One and two-dimensional inversion of MT data in continental regions. Phys. Earth Planet. Inter. 81, 155–176.
Aktas, K., Eaton, D.W., 2006. Upper-mantle velocity structure of the lower Great Lakes region. Tectonophysics 420, 267–281.
Artemieva, I.M., 2009. The continental lithosphere: reconciling thermal, seismic, and petrologic data. Lithos 109, 23–46.
Bahr, K., 1988. Interpretation of the magnetotelluric impedance tensor: regional induction and local telluric distortion. J. Geophys. 62, 119–127.
Benn, K., 2006. Tectonic delamination of the lower crust during Late Archean collision of the Abitibi–Opatica and Pontiac terranes, Superior Province, Canada. Archean Geodynamics and Environments. Geophysical Monograph Series 164. American Geophysical Union. http://dx.doi.org/10.1029/164GM17.
Benn, K., Miles, W., Ghassemi, M.R., Gillett, J., 1994. Crustal structure and kinematic framework of the northwestern Pontiac Subprovince, Quebec: an integrated structural and geophysical study. Can. J. Earth Sci. 31, 271–281.
Boerner, D.E., Kurtz, R.D., Craven, J.A., 2000. A summary of electromagnetic studies on the Abitibi–Grenville transect. Can. J. Earth Sci. 37, 427–437.
Cagniard, L., 1953. Basic theory of the magnetotelluric method of geophysical prospecting. Geophysics 18, 605–635.
Caldwell, T.G., Bibby, H.M., Brown, C., 2004. The magnetotelluric phase tensor. Geophys. J. Int. 158, 457–469.
Calvert, A.J., Ludden, J.N., 1999. Archean continental assembly in the southeastern Superior Province of Canada. Tectonics 18, 412–429.
Camire, G.E., Burg, J.-P., 1993. Late Archean thrusting in the northwestern Pontiac Subprovince, Canadian Shield. Precambrian Res. 61, 51–66.
Card, K.D., 1990. A review of the Superior Province of the Canadian shield, a product of Archean accretion. Precambrian Res. 48, 99–156.
Card, K.D., Ciesielski, A., 1986. Subdivisions of the Superior Province of the Canadian Shield. Geosci. Can. 13, 5–13.
Card, K.D., Poulsen, K.H., 1998. Geology and mineral deposits of the Superior Province of the Canadian shield. In: Lucas, S.B. (Ed.), Geology of the Precambrian Superior and Grenville Provinces and Precambrian Fossils in North America. Geology of Canada Series, No. 7. Geological Survey of Canada, pp. 13–194.
Carr, S.D., Easton, R.M., Jamieson, R.A., Culshaw, N.G., 2000. Geologic transect across the Grenville orogen of Ontario and New York. Can. J. Earth Sci. 37, 193–216.
Chave, A.D., Jones, A.G. (Eds.), 2012. The Magnetotelluric Method — Theory and Practice. Cambridge University Press, New York (570 pp.).
Chen, C.-W., Li, A., 2012. Shear wave structure in the Grenville Province beneath the lower Great Lakes region from Rayleigh wave tomography. J. Geophys. Res. 117, B01303.
Constable, S.C., 2006. SEO3: a new model of olivine electrical conductivity. Geophys. J. Int. 166, 435–437.
Constable, S.C., Shankland, T.J., Duba, A., 1992. The electrical conductivity of an isotropic olivine mantle. J. Geophys. Res. 97, 3397–3404.
Corrigan, D., van Breemen, O., 1997. U–Pb age constraints for the lithotectonic evolution of the Grenville Province along the Mauricie transect, Quebec. Can. J. Earth Sci. 34, 299–316.
Crough, S.T., 1981. Mesozoic hotspot epeirogeny in eastern North America. Geology 9, 2–6.
Culshaw, N.G., Davidson, A., Nadeau, L., 1983. Structural subdivisions of the Grenville Province in the Parry Sound–Algonquin region, Ontario. Current Research Part B, Geological Survey of Canada, paper 83-1B, pp. 243–252.
Culshaw, N.G., Jamieson, R.A., Ketchum, J.W.F., Wodicka, N., Corrigan, D., Reynolds, P.H., 1997. Transect across the northwestern Grenville orogen, Georgian Bay, Ontario: polystage convergence and extension in the lower orogenic crust. Tectonics 16, 966–982.
Daigneault, R., Mueller, W.U., Chown, E.H., 2004. Abitibi greenstone belt plate tectonics: the diachrononous history of arc development, accretion and collision. In: Eriksson, P., Altermann, W., Nelson, D., Mueller, W., Catuneanu, O. (Eds.), Tempos of Events in Precambrian Time. Developments in Precambrian Geology, Vol. 12. Elsevier, London, pp. 88 — 102–88 — .
Darbyshire, F.A., Eaton, D.W., Frederiksen, A.W., Ertolahti, L., 2007. New insights into the lithosphere beneath the Superior Province from Rayleigh wave dispersion and receiver function analysis. Geophys. J. Int. 169, 1043–1068.
Davidson, A., 1986. New interpretations in the southwestern Grenville Province. In: Moore, J.M., Davidson, A., Baer, A.J. (Eds.), The Grenville Province, Geological Association of Canada, Geological Survey of Canada, Special Paper 31, pp. 61–74.
Davidson, A., 1998. Questions of correlation across the Grenville Front east of Sudbury, Ontario. Current Research 1998-C; Geological Survey of Canada. Paper 98-IC, pp. 145–154.
Davidson, A., Morgan, W.C., 1981. Preliminary notes on the geology east of Georgian Bay, Grenville Structural Province, Ontario. Current Research, Geological Survey of Canada, Paper 81-1A, pp. 291–298.
Davidson, A., Culshaw, N.G., Nadeau, L., 1982. A tectono-metamorphic framework for part of the Grenville Province, Parry Sound region, Ontario. Current Research Part A, Geological Survey of Canada, paper 82-1A, pp. 175–190.
Demets, C., Gordon, R., Argus, D., Stein, S., 1990. Current plate motions. Geophys. J. Int. 101, 425–478.
Dickin, A.P., 2000. Crustal formation in the Grenville: Nd-isotope evidence. Can. J. Earth Sci. 37, 165–181.
Dimroth, E., Imreh, L., Rocheleau, M., Goulet, N., 1982. Evolution of the south-central segment of the Archean Abitibi Belt, Quebec, Part I, Stratigraphy and paleogeographic model. Can. J. Earth Sci. 19, 1729–1758.
Ducea, M.N., Park, S.K., 2000. Enhanced mantle conductivity from sulfide minerals, southern Sierra Nevada, California. Geophys. Res. Lett. 27, 2405–2408.
Easton, R.M., 1992. The Grenville Province and the Proterozoic history of Central and Southern Ontario. Geology of Ontario. Ontario Geological Survey, Special vol. 4, pp. 713–904.
Easton, R.M., Davidson, A., 1997. Frontenac–Sharbot Lake relationships: evaluation of a provocative hypothesis concerning the tectonics of the Central Metasedimentary Belt, Ontario. Friends of the Grenville, Annual Field Excursion Guidebook, pp. 26–28.
Eaton, D.W., Frederiksen, A., 2007. Seismic evidence for convection driven motion of the North American plate. Nature 446, 428–431.
Eaton, D.W., Adams, J., Asudeh, I., Atkinson, G.M., Bostock, M.G., Cassidy, J.F., Ferguson, I.J., Samson, C., Snyder, D.B., Tiampo, K.F., Unsworth, M.J., 2005. Geophysical arrays to investigate lithosphere and earthquake hazards in Canada. EOS Trans. AGU 86, 169–173.
Eaton, D.W., Dineva, S., Mereu, R., 2006. Crustal thickness and Vp/Vs variations in the Grenville orogen Ontario, Canada from analysis of teleseismic receiver functions. Tectonophysics 420, 223–238.
Evans, R.L., Jones, A.G., Garcia, X., Muller, M., Hamilton, M., Evans, S., Fourie, C.J.S., Spratt, J., Webb, S., Jelsma, H., Hutchins, D., 2011. Electrical lithosphere beneath the Kaapvaal craton, southern Africa. J. Geophys. Res. 116, B04105.
Faure, S., Godey, S., Fallara, F., Trepanier, S., 2011. Seismic architecture of the Archean North American mantle and its relationship to diamondiferous kimberlite fields. Econ. Geol. 106, 223–240.
Ferguson, I.J., Jones, A.G., Yu, S., Wu, X., Shiozaki, I., 1999. Geoelectric response and crustal electrical-conductivity structure of the Flin Flon Belt, Trans-Hudson Orogen, Canada. Can. J. Earth Sci. 36, 1917–1938.
Ferguson, I.J., Craven, J.A., Kurtz, R.D., Boerner, D.E., Bailey, R.C., Wu, X., Orellana, M.R., Spratt, J., Wennberg, G., Norton, M., 2005. Geoelectric responses of Archean lithosphere in the western Superior Province, central Canada. Phys. Earth Planet. Inter. 150, 123–143.
Ferguson, I.J., Jones, A.G., Chave, A.D., 2012. Case histories and geological applications. In: Chave, A.D., Jones, A.G. (Eds.), The Magnetotelluric Method: Theory and Practice. Cambridge University Press, New York, pp. 480–544.
Fischer, K.M., Ford, H.A., Abt, D.L., Rychert, C.A., 2010. The lithosphere–asthenosphere boundary. Annu. Rev. Earth Planet. Sci. 38, 551–575.
Fouch, M.J., Fischer, K.M., Parmentier, E.M., Wysession, M.E., Clarke, T.J., 2000. Shear wave splitting, continental keels, and patterns of mantle flow. J. Geophys. Res. 105, 6255–6275.

Frederiksen, A.W., Ferguson, I.J., Eaton, D., Miong, S.K., Gowan, E., 2006. Mantle fabric at multiple scales across an Archean–Proterozoic boundary, Grenville Front, Canada. Phys. Earth Planet. Inter. 158, 240–263.
Fullea, J., Muller, M.R., Jones, A.G., 2011. Electrical conductivity of continental lithospheric mantle from integrated geophysical and petrological modeling: application to the Kaapvaal Craton and Rehoboth Terrane, southern Africa. J. Geophys. Res. 116, B10202. http://dx.doi.org/10.1029/2011jb008544.
Glover, P.W.J., Vine, F.J., 1995. Beyond KTB — electrical conductivity of the deep continental crust. Surv. Geophys. 16, 5–36.
Gowan, E.J., Ferguson, I.J., Jones, A.G., Craven, J.A., 2009. Geoelectric structure of the northeastern Williston basin and underlying Precambrian lithosphere. Can. J. Earth Sci. 46, 441–464.
Green, A.G., Milkereit, B., Davidson, A., Spencer, C., Hutchinson, D.R., Cannon, W.F., Lee, M.W., Agena, W.F., Behrendt, J.C., Hinze, W.J., 1988. Crustal structure of the Grenville Front and adjacent terranes. Geology 16, 788–792.
Green, A.G., Cannon, W.F., Milkereit, B., Hutchinson, D.R., Davidson, A., Behrendt, J.C., Spencer, C., Lee, M.W., Morel-a-l'Huissier, P., Agena, W.F., 1989. A "Glimpce" of the deep crust beneath the Great Lakes, in properties and processes of Earth's lower crust. AGU Monogr. 51, 65–80. http://dx.doi.org/10.1029/GM051p0065.
Griffin, W.L., O'Reilly, S.Y., Doyle, B.J., Pearson, N.J., Coopersmith, H., Kivi, K., Malkovets, V., Pokhilenko, N., 2004. Lithosphere mapping beneath the North American plate. Lithos 77, 873–922.
Gripp, A.E., Gordon, R.G., 2002. Young tracks of hotspots and current plate velocities. Geophys. J. Int. 150, 321–361.
Groom, R.W., Bailey, R.C., 1989. Decomposition of magnetotelluric impedance tensors in the presence of local three-dimensional galvanic distortion. J. Geophys. Res. 94, 1913–1925.
Groom, R.W., Bailey, R.C., 1991. Analytic investigations of the effects of near-surface three-dimensional glavanic scatterers on MT tensor decompositions. Geophysics 56, 496–518.
Haggart, M.J., Jemieson, R.A., Reynold, P.H., Krogh, T.E., Beaumont, C., Culshaw, N.G., 1993. Last gasp of the Grenville Orogeny: thermochronology of the Grenville Front Tectonic Zone near Killarney, Ontario. J. Geol. 101, 575–589.
Hamilton, M.P., Jones, A.G., Evans, R.L., Evans, S., Fourie, C.J.S., Garcia, X., Mountford, A., Spratt, J.E., the SAMTEX Team, 2006. Electrical anisotropy of South African lithosphere compared with seismic anisotropy from shear-wave splitting analysis. Phys. Earth Planet. Inter. 158, 226–239.
Hanmer, S., 1988. Ductile thrusting at mid-crustal level, southwestern Grenville Province, Canada. Can. J. Earth Sci. 25, 1049–1059.
Hanmer, S., Ciesielski, A., 1984. A structural reconnaissance of the northwest boundary of the Central Metasedimentary Belt, Grenville Province, Ontario and Quebec. Current Research Part B, Geological Survey of Canada, Paper 84-18, pp. 121–131.
Hanmer, S., McEachern, S.J., 1992. Kinematical and rheological evolution of a crustal-scale ductile thrust zone, Central Metasedimentary Belt, Grenville Orogen, Canada. Can. J. Earth Sci. 29, 1779–1790.
Hanmer, S., Thivierge, R.H., Henderson, J.R., 1985. Anatomy of a ductile thrust zone: part of the northwest boundary of the Central Metasedimentary Belt, Grenville Province, Ontario. Current Research Part B, Geological Survey of Canada, Paper 85-18, pp. 1–5.
Hildebrand, R.S., Easton, R.M., 1995. A 1161 Ma suture in the Frontenac terrane, Ontario segment of the Grenville orogeny. Geology 23, 917–920.
Hirth, G., Evans, R.L., Chave, A.D., 2000. Comparison of continental and oceanic mantle electrical conductivity: is the Archean lithosphere dry? Geochem. Geophys. Geosyst. 1, 1030. http://dx.doi.org/10.1029/2000GC000048.
Hoffman, P.F., 1989. Precambrian geology and tectonic history of North America. In: Bally, A.W., Palmer, A.R. (Eds.), The geology of North America — An Overview. The Geological Society of America, vol. A, pp. 447–512.
Hyndman, R.D., Wang, K., Yuan, T., Spence, G.D., 1993. Tectonic sediment thickening, fluid expulsion, and the thermal regime of subduction zone accretionary prisms: the Cascadia margin off Vancouver Island. J. Geophys. Res. 98, 21865–21876. http://dx.doi.org/10.1029/93JB02391.
Hynes, A., Rivers, T., 2010. Protracted continental collision — evidence from the Grenville Orogen. Can. J. Earth Sci. 47, 591–620.
Ji, S., Rondenay, S., Mareschal, M., Senechal, G., 1996. Obliquity between seismic and electrical anisotropies as a potential indicator of movement sense for ductile shear zones in the upper mantle. Geology 24, 1033–1036.
Jödicke, H., Jording, A., Ferrari, L., Arzate, J., Mezger, K., Rüpke, L., 2006. Fluid release from the subducted Cocos plate and partial melting of the crust deduced from magnetotelluric studies in southern Mexico: implications for the generation of volcanism and subduction dynamics. J. Geophys. Res. 111, B08102. http://dx.doi.org/10.1029/2005JB003739.
Jones, A.G., 1983. On the equivalence of the "Niblett" and "Bostick" transformations in the magnetotelluric method. J. Geophys. 53, 72–73.
Jones, A.G., 1988. Static shift of magnetotelluric data and its removal in a sedimentary basin environment. Geophysics 53, 967–978.
Jones, A.G., 1992. Electrical conductivity of the continental lower crust. In: Fountain, D.M., Arculus, R.J., Kay, R.W. (Eds.), Continental Lower Crust. Elsevier, Amsterdam, pp. 81–143.
Jones, A.G., 1999. Imaging the continental upper mantle using electromagnetic methods. Lithos 48, 57–80.
Jones, A.G., 2006. Electromagnetic interrogation of the anisotropic Earth: looking into the Earth with polarized spectacles. Phys. Earth Planet. Inter. 158, 281–291.
Jones, A.G., 2012. Distortion of magnetotelluric data: its identification and removal. In: Chave, A.D., Jones, A.G. (Eds.), The Magnetotelluric Method: Theory and Practice. Cambridge University Press, New York, pp. 219–295.
Jones, A.G., Craven, J.A., 1990. The North American Central Plains conductivity anomaly and its correlation with gravity, magnetic, seismic, and heat flow data in Saskatchewan, Canada. Phys. Earth Planet. Inter. 60, 169–194.
Jones, A.G., Craven, J.A., 2004. Area selection for diamond exploration using deep-probing electromagnetic surveying. Lithos 77, 765–782.
Jones, A.G., Savage, P.J., 1986. North American Central Plains conductivity anomaly goes east. Geophys. Res. Lett. 13, 685–688.
Jones, A.G., Katsube, J., Schwann, P., 1997. The longest conductivity anomaly in the world explained: sulphides in fold hinges causing very high electrical anisotropy. J. Geomagn. Geoelectr. 49, 1619–1629.
Jones, A.G., Ferguson, I.J., Chave, A.D., Evans, R.L., McNeice, G.W., 2001. The electric lithosphere of the Slave craton. Geology 29, 423–426.
Jones, A.G., Snyder, D., Hanmer, S., Asudeh, I., White, D., Eaton, D., Clarke, G., 2002. Magnetotelluric and teleseismic study across the Snowbird Tectonic Zone, Canadian Shield: a Neoarchean mantle suture? Geophys. Res. Lett. 29. http://dx.doi.org/10.1029/2002GL015359.
Jones, A.G., Lezaeta, P., Ferguson, I.J., Chave, A.D., Evans, R.L., Garcia, X., Spratt, J., 2003. The electrical structure of the Slave craton. Lithos 71, 505–527.
Jones, A.G., Evans, R.L., Eaton, D.W., 2009a. Velocity-conductivity relationships for mantle mineral assemblages in Archean cratonic lithosphere based on a review of laboratory data and Hashin–Shtrikman extremal bounds. Lithos 109, 131–143. http://dx.doi.org/10.1016/j.lithos.2008.10.014.
Jones, A.G., Evans, R.L., Muller, M.R., Hamilton, M.P., Miensopust, M.P., Garcia, X., Cole, P., Ngwisanyi, T., Hutchins, D., Fourie, C.J.S., Jelsma, H., Evans, S., Aravanis, T., Pettit, W., Webb, S., Wasborg, J., The, S.A.M.T.E.X., 2009b. Area selection for diamonds using magnetotellurics: examples from southern Africa. Lithos 112, 83–92.
Jones, A.G., Plomerova, J., Korja, T., Sodoudi, F., Spakman, W., 2010. Europe from the bottom up: a statistical examination of the central and northern European lithosphere–asthenosphere boundary from comparing seismological and electromagnetic observations. Lithos 120, 14–29.
Kamo, S.L., Krogh, T.E., Kumarapeli, P.S., 1995. Age of the Grenville dyke swarm, Ontario–Quebec: implications for the timing of Iapetan rifting. Can. J. Earth Sci. 32, 273–280.
Karato, S., 1990. The role of hydrogen in the electrical conductivity of the upper mantle. Nature 347, 272–273.
Karato, S.I., 2012. On the origin of the asthenosphere. Earth Planet. Sci. Lett. 321, 95–103.
Katsube, T.J., Mareschal, M., 1993. Petrophysical model of deep electrical conductors: graphite lining as a source and its disconnection due to uplift. J. Geophys. Res. 98, 8019–8083.
Kellett, R.L., Mareschal, M., Kurtz, R.D., 1992. A model of lower crustal electrical anisotropy for the Pontiac Subprovince of the Canadian Shield. Geophys. J. Int. 111, 141–150.
Kellett, R.L., Barnes, A.E., Rive, M., 1994. The deep structure of the Grenville Front: a new perspective from western Quebec. Can. J. Earth Sci. 31, 282–292.
Kerrich, R., Ludden, J., 2000. The role of fluids during formation and evolution of the southern Superior Province lithosphere: an overview. Can. J. Earth Sci. 37, 135–164.
Korja, T., 2007. How is the European lithosphere imaged by magnetotellurics? Surv. Geophys. 28, 239–272.
Korja, T., Tuisku, P., Pernu, T., Karhu, J., 1996. Lapland Granulite Belt — implications for properties and evolution of deep continental crust. Terra Nova 8, 48–58.
Korja, T., Engels, M., Zhamaletdinov, A.A., Kovtun, A.A., Palshin, N.A., Smirnov, M.Yu, Tokarev, A., Asming, V.E., Vanyan, L.L., Vardaniants, I.L., the BEAR Working Group, 2002. Crustal conductivity in Fennoscandia — a compilation of a database on crustal conductance in the Fennoscandian Shield. Earth Planets Space 54, 535–558.
Krogh, T.E., 1994. Precise U–Pb ages for Grenvillian and pre-Grenvillian thrusting of Proterozoic and Archean metamorphic assemblages in the Grenville Front Tectonic Zone, Canada. Tectonics 13, 963–982.
Kumarapeli, P.S., 1985. Vestiges of Iapetan rifting in the craton west of Appalachians. Geosci. Can. 12, 54–59.
Kurtz, R.D., 1982. Magnetotelluric interpretation of crustal and mantle structure in the Grenville Province. Geophys. J. R. Astron. Soc. 70, 373–397.
Kurtz, R.D., Craven, J.A., Niblett, E.R., Stevens, R.A., 1993. The conductivity of the crust and mantle beneath the Kapuskasing Uplift: electrical anisotropy in the upper mantle. Geophys. J. Int. 113, 483–498.
Larson, K.M., Freymueller, J.T., Philipsen, S., 1997. Global plate velocities from the Global Positioning System. J. Geophys. Res. 102, 9961–9981.
Ledo, J., Queralt, P., Marti, A., Jones, A.G., 2002. Two-dimensional interpretation of three-dimensional magnetotelluric data: an example of limitations and resolution. Geophys. J. Int. 150, 127–139.
Ledo, J., Jones, A.G., Ferguson, I.J., Wolynec, L., 2004. Lithospheric structure of the Yukon, northern Canadian Cordillera obtained from magnetotelluric data. J. Geophys. Res. 109, B04410. http://dx.doi.org/10.1029/2003JB002516.
Li, S., Unsworth, M.J., Booker, J.B., Wei, W., Tan, H., Jones, A.G., 2003. Partial melt or aqueous fluid in the mid-crust of Southern Tibet? Constraints from INDEPTH Magnetotelluric data. Geophysics 153, 289–304.
Ludden, J., Hubert, C., 1986. Geologic evolution of the Late Archean Abitibi Greenstone Belt of Canada. Geology 14, 707–711.
Ludden, J., Hynes, A., 2000. The Lithoprobe Abitibi–Grenville transect: two billion years of crust formation and recycling in the Precambrian Shield of Canada. Can. J. Earth Sci. 37, 459–476.
Mackie, R., Rieven, S., Rodi, W., 1997. Users Manual and Software Documentation for Two-Dimensional Inversion of Magnetotelluric Data. GSY-USA, San Francisco (14 pp.).
Mareschal, M., Kellett, R.L., Kurtz, R.D., Ludden, J.N., Ji, S., Bailey, R.C., 1995. Archean cratonic roots mantle shear zones and deep electrical anisotropy. Nature (London) 375, 134–137.
Martignole, J., Calvert, A.J., 1996. Crustal-scale shortening and extension across the Grenville Province of western Quebec. Tectonics 15, 376–386.
McNeice, G.W., Jones, A.G., 2001. Multisite, multifrequency tensor decomposition of magnetotelluric data. Geophysics 56, 158–173.

Mereu, R.F., Wang, D., Kuhm, O., 1986. The 1982 COCRUST seismic experiment across the Ottawa–Bonnechere graben and Grenville Front in Ontario and Quebec. Geophys. J. R. Astron. Soc. 84, 491–514.
Meyer, H.O.A., Waldman, M.A., Garwood, B.L., 1994. Mantle xenoliths from kimberlite near Kirkland Lake, Ontario. Can. Min. 32, 295–306.
Mibe, K., Fuji, T., Yasuda, A., 1998. Connectivity of aqueous fluid in the Earth's upper mantle. Geophys. Res. Lett. 25, 1233–1236.
Miensopust, M.P., Jones, A.G., Muller, M.R., Garcia, X., Evans, R.L., 2011. Lithospheric structures and Precambrian terrane boundaries in northeastern Botswana revealed through magnetotelluric profiling as part of the Southern African Magnetotelluric Experiment. J. Geophys. Res. 116, B02401.
Muller, M.R., Jones, A.G., Evans, R.L., Gru¨tter, H.S., Hatton, C., Garcia, X., Hamilton, M.P., Miensopust, M.P., Cole, P., Ngwisanyi, T., Hutchins, D., Fourie, C.J., Jelsma, H.A., Evans, S.F., Aravanis, T., Pettit, W., Webb, S.J., Wasborg, J., The SAMTEX Team, 2009. Lithospheric structure, evolution and diamond prospectivity of the Rehoboth Terrane and the western Kaapvaal Craton, southern Africa: constraints from broadband magnetotellurics. Lithos 112S, 93–105.
Niblett, E.R., Sayn-Wittgenstein, C., 1960. Variation of electrical conductivity with depth by the magneto-telluric method. Geophysics 25, 998–1008.
Nover, G., Heikamp, S., Meurer, H.J., Freund, D., 1998. In-situ electrical conductivity and permeability of mid-crustal rocks from the KTB drilling: consequences for high conductive layers in the earth crust. Surv. Geophys. 19, 73–85.
O'Dowd, C.R., Eaton, D., Forsyth, D., Asmis, H.W., 2004. Structural fabric of the Central Metasedimentary Belt of southern Ontario, Canada, from deep seismic profiling. Tectonophysics 388, 145–159.
Park, S.K., Mackie, R.J., 1997. Crustal structure at Nanga Parbat, northern Pakistan, from magnetotelluric soundings. Geophys. Res. Lett. 24, 2415–2418.
Parker, R.L., 1980. The inverse problem of electromagnetic induction: existence and construction of solutions based on incomplete data. J. Geophys. Res. 85, 4421–4425.
Parker, R.L., Booker, J.R., 1996. Optimal one-dimensional inversion and bounding of magnetotelluric apparent resistivity and phase measurements. Phys. Earth Planet. Inter. 98, 269–282.
Percival, J.A., Bleeker, W., Cook, F.A., Rivers, T., Ross, G., van Staal, C., 2004. PanLITHOPROBE Workshop IV: intra-orogen correlations and comparative orogenic anatomy. Geosci. Can. 31, 23–39.
Rivers, T., 1997. Lithotectonic elements of the Grenville Province: review and tectonic implications. Precambrian Res. 86, 117–154.
Rivers, T., Martignole, J., Gower, C.F., Davidson, A., 1989. New tectonic subdivisions of the Grenville Province, southeast Canadian Shield. Tectonics 8, 63–84.
Rodi, W.L., Mackie, R.L., 2001. Nonlinear conjugate gradients algorithm for 2D magnetotelluric inversion. Geophysics 66, 174–187.
Rodi, W.L., Mackie, R.L., 2012. The inverse problem. In: Chave, A.D., Jones, A.G. (Eds.), The Magnetotelluric Method: Theory and Practice. Cambridge University Press, New York, pp. 347–414.
Rondenay, S., Bostock, M.G., Hearn, T.M., White, D.J., Ellis, R.M., 2000. Lithospheric assembly and modification of SE Canadian Shield: Abitibi–Grenville teleseismic experiment. J. Geophys. Res. 105, 13735–13754.
Roy, B., Mereu, R.F., 2000. Applications of seismic pattern recognition and gravity inversion techniques to obtain enhanced subsurface images of the Earth's crust under the Central Metasedimentary Belt, Grenville Province, Ontario. Geophys. J. Int. 143, 735–751.
Schäfer, A., Houpt, L., Brasse, H., Hoffmann, N., EMTESZ Working Group, 2011. The North German Conductivity Anomaly revisited. Geophys. J. Int. 187, 85–98.
Schwarz, G., 1990. Electrical conductivity of the earth's crust and upper mantle. Surv. Geophys. 11, 133–161.
Selway, K., 2013. On the causes of electrical conductivity anomalies in tectonically stable lithosphere. Surv. Geophys.. http://dx.doi.org/10.1007/s10712-013-9235-1.
Sénéchal, G., Rondenay, S., Mareschal, M., Guilbert, J., Poupinet, G., 1996. Seismic and electrical anisotropies in the lithosphere across the Grenville Front, Canada. Geophys. Res. Lett. 23, 2255–2258.
Simpson, F., 2001. Resistance to mantle flow inferred from the electromagnetic strike of the Australian upper mantle. Nature 412, 632–633.
Simpson, F., Bahr, K., 2005. Practical Magnetotellurics. Cambridge University Press, Cambridge, United Kingdom (254 pp.).
Sleep, N.H., 1990. Monteregian hotspot track: a long-lived mantle plume. J. Geophys. Res. 95, 21,983–21,990.
Snyder, D., Grütter, H.S., 2010. Lithoprobe's impact on the Canadian diamond-exploration industry. Can. J. Earth Sci. 47, 783–800.
Soyer, M., Unsworth, M., 2006. Deep electrical structure of the northern Cascadia British Columbia, Canada) subduction zone: implications for the distribution of fluids. Geology 34, 53–56.
Spratt, J.E., Jones, A.G., Jackson, V.A., Collins, L., Avdeeva, A., 2009. Lithospheric geometry of the Wopmay orogen from a Slave craton to Bear Province magnetotelluric transect. J. Geophys. Res. 114, B01101.
Tikhonov, A.N., 1950. The determination of the electrical properties of the deep layers of the Earth's crust. Dokl. Acad. Nauk SSR 73, 295–297 (in Russian).
van der Lee, S., Nolet, G., 1997. Upper mantle S velocity structure of North America. J. Geophys. Res. 102, 22,815–22,838.
Vozoff, K., 1991. The magnetotelluric method. In: Nabighian, M.N. (Ed.), Electromagnetic Methods in Applied Geophysics. Society of Exploration Geophysicist, pp. 641–711.
Weidelt, P., Chave, A.D., 2012. The magnetotelluric response function. In: Chave, A.D., Jones, A.G. (Eds.), The Magnetotelluric Method: Theory and Practice. Cambridge University Press, New York, pp. 122–162.
White, D.J., Forsyth, D.A., Asudeh, I.A., Carr, S.D., Wu, H., Easton, R.M., Mereu, R.F., 2000. A seismic-based cross-section of the Grenville Orogen in Southern Ontario and western Quebec. Can. J. Earth Sci. 37, 183–192.
Wu, X., Ferguson, I.J., Jones, A.G., 2002. Magnetotelluric response and geoelectric structure of the Great Slave Lake Shear Zone. Earth Planet. Sci. Lett. 196, 35–50.
Xu, Y.S., Shankland, T.J., 1999. Electrical conductivity of orthopyroxene and its high pressure phases. Geophys. Res. Lett. 26, 2645–2648.
Xu, Y.S., Shankland, T.J., Duba, A.G., 2000. Pressure effect on electrical conductivity of mantle olivine. Phys. Earth Planet. Inter. 118, 149–161.
Yoshino, T., Manthilake, G., Matsuzaki, T., Katsura, T., 2008. Dry mantle transition zone inferred from the conductivity of wadsleyite and ringwoodite. Nature 451, 326–329.
Zhang, J., Frederiksen, A.W., 2013. 3-D crust and mantle structure in Southern Ontario, Canada via receiver function imaging. Tectonophysics 608, 700–712.
Zhang, P., Pedersen, L.B., Mareschal, M., Chouteau, M., 1993. Channelling contribution to tipper vectors: a magnetic equivalent to electrical distortion. Geophys. J. Int. 113, 693–700.
Zhang, P., Chouteau, M., Mareschal, M., Kurtz, R.D., Hubert, C., 1995. High frequency magnetotelluric investigation of crustal structure in north-central Abitibi, Quebec, Canada. Geophys. J. Int. 120, 406–418.